

**Soluble LRP6 E1-E2 Wnt receptor to
regulate tumor growth and
cellular invasion**

Jung-Sun Lee

Department of Medical Science

The Graduate School, Yonsei University

**Soluble LRP6 E1-E2 Wnt receptor to
regulate tumor growth and
cellular invasion**

Jung-Sun Lee

Department of Medical Science

The Graduate School, Yonsei University

**Soluble LRP6 E1-E2 Wnt receptor to
regulate tumor growth and
cellular invasion**

Directed by Professor Man-Wook Hur

**The doctoral Dissertation submitted to the Department of
Medical Science,
the Graduate School of Yonsei University in partial
fulfillment of the requirements for the degree of
Doctor of Philosophy Medical Science**

Jung-Sun Lee

June 2012

**This certifies that the doctoral
dissertation of Jung-Sun Lee is
approved**

Thesis Supervisor : Man-Wook Hur

Thesis Committee Member #1: Chea-Ok Yun

Thesis Committee Member #2: Si Young Song

Thesis Committee Member #3: Jeon Han Park

Thesis Committee Member #4: Kyung-Sup Kim

The Graduate School

Yonsei University

June 2012

ACKNOWLEDGEMENTS

지난 5년간의 시간들이 주마 등처럼 스쳐 지나갑니다. 처음 암연구소 철문의 초인종을 누르면서 다짐했던 나와 의 약속과 도전들..... 그리고 이제 그 결실을 마치면서 그간 고마웠던 마음들을 이 지면을 빌어 전하고자 합니다

먼저 제가 이 자리에 있기까지 이정선 다운 저를 만들어 주신 가장 존경하는 윤채욱 교수님께 진심으로 머리 숙여 감사의 말을 전하고 싶습니다. 학문적으로나 한 사람으로써의 부족한 점을 일깨워 주셔서 저를 성숙하게 만들어 주신 분은 교수님입니다. 인생의 스승으로써의 주옥 같은 말씀들 가슴 깊이 새기도록 하겠습니다. 선생님께서 저에게 주신 모든 열정과 노력들이 헛되지 않도록 제 삶에 최선을 다하도록 노력하겠습니다. 그리고 저를 아껴주시고 격려해 주신 허만욱 교수님께도 감사의 마음을 전하고 싶습니다. 항상 열린 마음으로 많은 가르침과 조언을 해주시고 과학자로서의 자질에 대한 여러가지 주옥 같은 말씀들 가슴 깊이 새기도록 하겠습니다. 바쁘신 시간에도 논문에 대한 관심과 열정 그리고 논문이 나아가야 할 방향들을 세심하게 지도해 주셨던 송시영 교수님, 제가 미처 보지 못한 분야에 눈을 뜨게 해주시고 잘못 알고 있던 내용을 바로 잡아주시며 세심하게 학위 심사를 해주신 김경섭 교수님, 그리고 이번 학위를 하면서 가장 논문에 대한 많은 애정과 관심을 가져주시고 박사 학위에 대한 참 뜻 그리고 소양을 일깨워 주신 박전한 교수님께 진심으로 감사의 마음을 전하고 싶습니다. 학위 하는 동안 제가 이렇게 훌륭한 교수님들을 만나 배웠다는 것이 저에게 있어서 정말 큰 행운이자 학문의 즐거움이었다고 말씀 드리고 싶습니다.

아무리 좋은 농부가 있어도 토양이 비옥하지 않으면 열매가 열릴 수 없듯이 저에게 그 무엇보다도 좋은 토양이 되어 주었던 우리 실험실 식구들에게 감사의 말을 전하고 싶습니다. 모든 일에 정말 최고였던 지영언니, 말하지 않은 것도 마음 깊이 알아주고 항상 격려해 주셨던 경주언니, 항상 따뜻한 말로, 또한 따듯한 충고로 일깨워 주셨던 민정언니. 동갑이지만, 선배 같았던 아름이. 모르는 것이 없는 만능 박사 김인욱 선생님, 그리고 지금은 안 계시지만 모르는 것이 있으면 늘 자상하게 가르쳐 주고 너무나 잘 이해 주었던 강은아 선생님, 그리고 영어에 대한 어려움을 항

상 해결해 주신 카살라 선생님, 나에게도 동생이지만 배울 점이 많고 학문적 즐거움을 주었던 일규, 어른스럽고 자신의 일도 척척 잘하는 오준이, 그리고 많은 자극제가 되었고 지금은 너무나 자랑스러운 송남이. 이런 훌륭한 선배님들이 이룩한 모든 것들이 헛되지 않도록 노력하겠습니다. 그리고 그간 동고동락 하면서 많은 일들을 겪었던 정말 소중한 동기와 후배들에게도 고마움을 전하고 싶습니다. 나와 동기 그러기에 더 많이 의지하였던 지훈오빠, 마음은 한없이 여리고 어린 아이 같지만 속 깊고 일도 잘 하는 정우, 팔 씨름으로 친해졌지만 유머감각, 클로닝이 뛰어난 리연 (나만의 애칭 연희~), 가장 많이 혼내서 마음이 아프지만 그만큼 애정이 가는 후배 성경이, 가슴 애련하고 그래서 더욱 보살펴 주고 싶은 유진, 너무 똑 소리나게 일을 잘하는 언주, 서글서글한 웃음과 항상 뭐든지 열심히 하는 초희, 실험실의 일꾼이자 기대주 효민, 먼 곳에 와 적응하느라 힘들 텐데 뭐든지 정말 열심히 해주어서 고마운 해단이, 막내지만 그만큼 열심히 하고 억척스러운 수정, 그리고 너무 예의 바른 선배들 따라다니며 열심히 배우는 종현이.. 지금은 졸업해서 이 자리에 없지만 나의 학교 후배이자 미국에서 열심히 공부하고 있을 혜원이, 속 깊고 만나면 편한 친구 같은 후배 지성, 처음 실험실에 들어와 많이 도와주고 가장 친했던 야기 엄마 민주, 고집이 있어 언젠가 정말 빛을 발휘할 것이라 생각이 드는 부산 사나이 태진. 이런 훌륭한 후배님들이 계시기에 앞으로 실험실이 더욱더 빛날 것이라는 생각이 듭니다.

대학 때부터 항상 내 곁에서 나를 묵묵히 응원해준 나의 소중한 친구들 (태현, 영미, 혜진, 소용, 정연, 은정), 늘 어린 후배여서 보살펴 주고 아낌없이 조언을 해주던 예선언니, 시화선배, 가끔씩 투정부리지만 귀여운 내 후배들 (보영, 영재, 미영) 그리고 마지막으로 항상 내편에서 서서 내가 힘들 때나 어려울 때 내 눈물을 진심으로 닦아주고 어루만져 주었던 인생에 가장 소중한 친구 보경에게 진심으로 감사드립니다. 사실 인생살이가 그렇듯 늘 긴장 속에서 살아가는데 좋은 친구들이 있기에 기댈 곳이 있었던 것 같습니다. 감사 드립니다.

그리고 이 세상에서 가장 소중한 가족들 에게 감사 드립니다. 학위 하는 동안에 묵묵히 지원해준 남편 한필승, 공부하는데 여러모로 도와주시고 많이 이해해 주신 시부모님에게 고마움과 감사함을 전합니다. 또한, 항상 저를 뒷바라질 하느라 당신의

인생까지 희생하신 저희 소중한 엄마 이경숙 여사께 진심으로 감사 드립니다. 공부
한답시고 언니로써 제대로 역할을 하지 못했지만 묵묵히 도와주고 늘 힘이 해주었
던 나의 사랑스런 동생들 효선, 혜선에게 미안함과 감사함을 전합니다. 마지막으로
나의 소중한 보물 이자 나의 삶 전체인 아들 한준모, 딸을 자랑스럽게 생각하실 아
버지 영전에 이 논문을 바칩니다.

이 감사의 글을 마지막으로 전 여기에 머물지 않고 다시 새롭게 더 열심히 달리려
고 합니다. 결코 이것이 끝이 아니라 시작이기에 어떤 일들이 제게 펼쳐질지 벌써
부터 기대됩니다.

무더운 여름날 밤에 감사의 글을 전하며

TABLE OF CONTENTS

ABSTRACT.....	1
I. INTRODUCTION.....	3
II. MATERIALS AND METHODS.....	6
1. Ethics Statement.....	6
2. Materials	6
3. Cell lines and culture conditions	7
4. Luciferase reporter assay for β -catenin activity	8
5. Cell proliferation assay	9
6. Western blotting	9
7. Immunofluorescence assay	10
8. Mitochondrial fractionation and western blotting	10
9. Anti-tumor effects in xenograft model.....	11
10. Tumor histology and immunohistochemistry	12
11. Terminal deoxynucleotidyl transferase dUTP nick end labeling assay	13
12. Migration and invasion assay	14
13. Statistical analysis	15

III. RESULTS

1. Generation of adenoviral vectors expressing soluble LRP6 receptor	16
2. Soluble Wnt decoy receptor is expressed in lung cancer cell lines and binds to Wnt3a	17
3. Soluble Wnt decoy receptor binds to Wnt3a	18
4. Decoy Wnt receptor decreases cytosolic β -catenin level and TCF transcriptional activity	20
5. Decoy Wnt receptor sLRP6E1E2 inhibits lung cancer cell proliferation.....	25
6. Decoy Wnt receptor sLRP6E1E2 down-regulated both the Wnt and ERK,PI3K pathways.....	27
7. Decoy Wnt receptor sLRP6E1E2 induces apoptosis	28
8. Decoy Wnt receptor sLRP6E1E2 increased cytochrome c-dependent caspase activation	30
9. Decoy Wnt receptor sLRP6E1E2 inhibits lung tumor xenograft growth	33
10. Anti-proliferative and apoptotic effects of sLRP6E1E2-expressing vectors in H460 xenografts.....	35
11. Decoy Wnt receptor sLRP6E1E2 inhibits breast tumor xenograft	

growth	37
12. Decoy Wnt receptor sLRP6E1E2 decrease stem cell property of mice bearing breast xenografts	39
13. Wnt treatment results altered cell morphology and induces EMT in tumor cells.....	41
14. sLRP6E1E2 suppresses in vitro motility and invasiveness.....	43
15. sLRP6E1E2 modulates EMT-related marker expression and MMP 2/MMP-9 activity	45
IV. DISCUSSION	50
V. CONCLUSION	54
REFERENCES	55
VI. ABSTRACT (IN KOREAN)	63

LIST OF FIGURES

Figure 1.	Constructs of the adenoviral (Ad) vector	17
Figure 2.	Characterization of the decoy Wnt receptor sLRP6E1E2	18
Figure 3.	Soluble Wnt decoy receptor binds to Wnt3a	20
Figure 4.	Decoy Wnt receptor sLRP6E1E2 reduces T-cell factor transcriptional activity.....	22
Figure 5.	Effect of Decoy Wnt receptor sLRP6E1E2 on β -catenin localization	25
Figure 6.	Decoy Wnt receptor sLRP6E1E2 decreases proliferation in human lung cancer cell.....	26
Figure 7.	Decoy Wnt receptor sLRP6E1E2 decreases Wnt signaling and MEK-ERK and PI3K- Akt signaling.....	28
Figure 8.	Decoy Wnt receptor sLRP6E1E2 induces apoptosis in human lung cancer cells	30
Figure 9.	Decoy Wnt receptor sLRP6E1E2 regulate the release of apoptogenic cytochrome c	32
Figure 10.	Decoy Wnt receptor sLRP6E1E2 inhibit <i>in vivo</i> tumor growth.....	34
Figure 11.	Histological characterization of tumor tissue in H460	

	xenografts	37
Figure 12.	Anti-tumor effects of decoy Wnt receptor sLRP6E1E2...	38
Figure 13.	Decoy Wnt receptor sLRP6E1E2 are decreased enriched breast cancer cell for tumorigenicity	40
Figure 14.	Wnt3a treatment results in the disruption of cell-cell junctions and epithelial-to-mesenchymal transition in tumor cells	42
Figure 15.	Inhibition of cancer cell migration and invasion by Decoy Wnt receptor sLRP6E1E2	44
Figure 16.	Decoy Wnt receptor sLRP6E1E2 modulates expression of epithelial-to-mesenchymal transition markers and MMPs	48

ABSTRACT

Soluble LRP6 E1-E2 Wnt receptor to regulate tumor growth and cellular invasion

Jung-Sun Lee

Department of Medical Science

The Graduate School, Yonsei University

(Directed by Professor **Man-Wook Hur**)

Aberrant activation of the Wnt pathway contributes to human cancer progression. Antagonists that interfere with Wnt ligand/receptor interactions can be useful in cancer treatments. In this study, we evaluated the therapeutic potential of a soluble Wnt receptor decoy in cancer gene therapy. We designed a Wnt antagonist sLRP6E1E2, and generated a replication-incompetent adenovirus (Ad), dE1-k35/sLRP6E1E2, and a replication-competent oncolytic Ad, RdB-k35/sLRP6E1E2, both expressing sLRP6E1E2. sLRP6E1E2 prevented Wnt-mediated stabilization of cytoplasmic β -catenin, decreased Wnt/ β -catenin signaling and cell proliferation via the mitogen-activated

protein kinase, and phosphatidylinositol 3-kinase pathways. sLRP6E1E2 induced apoptosis, Cytochrome *c* release, and increased cleavage of PARP and caspase-3. sLRP6E1E2 suppressed growth of the human tumor xenograft, reduced motility and invasion of cancer cells. In addition, sLRP6E1E2 upregulated expression of epithelial marker genes, while sLRP6E1E2 downregulated mesenchymal and differentiation markers genes. Taken together, sLRP6E1E2, by inhibiting interaction between Wnt and its receptor, suppressed Wnt-induced cell proliferation and epithelial-to-mesenchymal transition

Key words: Wnt, soluble Wnt decoy receptor, LRP6, β -catenin, Cancer, epithelial-to-mesenchymal transition (EMT), cell proliferation, apoptosis

Soluble LRP6 E1-E2 Wnt receptor to regulate tumor growth and cellular invasion

Jung-Sun Lee

Department of Medical Science

The Graduate School, Yonsei University

(Directed by Professor **Man-Wook Hur**)

I. INTRODUCTION

Aberrant activation of the Wnt signaling pathway is implicated in the development of a broad spectrum of tumors ¹. Standard therapies such as surgery and radiation are not effective in many cases ². However, an increased understanding of the molecular mechanisms of cancer has led to the development of promising new therapies ³. Although chemotherapy advances have improved overall survival for patients with aggressive cancer, chemoresistance remains a major cause of treatment failure ⁴. Many aggressive cancers show alterations in various cancer-associated genes, including Wnt, K-ras, extracellular signal-regulated kinase (ERK), Akt, and

cyclooxygenase-2, suggesting a different molecular pathway for carcinogenesis in lung adenocarcinomas⁵⁻⁷.

The role of Wnt signaling in cancer was first suggested 20 years ago with the discovery of Wnt-1 as an integration site for mouse mammary tumor virus⁸. Many studies have reported that altered expression of Wnt ligands, receptors, and extracellular antagonists are associated with cancer development/progression and stem cell self-renewal/differentiation⁹. Expression of the Wnt ligand, low-density lipoprotein receptor-related protein 5 (LRP5), and LRP6 are upregulated in cancers, whereas Wnt antagonists that bind Wnt ligands to block interaction with receptors (e.g., Wnt inhibitory factor-1 (WIF-1), secreted Frizzled-related proteins (sFRP) and dickkopf proteins (DKK) are downregulated or inactivated^{10,11}. Accordingly, monoclonal antibodies and small interfering RNAs against Wnt and overexpression of Wnt antagonists suppress tumor growth in various *in vitro* and *in vivo* tumor models.

LRP6, a member of the LRP superfamily, is required for activation of the canonical Wnt signaling pathway, which leads to the stabilization and nuclear translocation of β -catenin, the key effector molecule¹². LRP6 consists of four distinct YWTD β -propeller/EGF-like domain pairs; the first and second YWTD domains (E1 and E2) are required for binding to Wnt¹³⁻¹⁵. In

the present study, we explored the therapeutic potential of a novel soluble Wnt receptor, sLRP6E1E2, which is composed of the LRP6 E1 and E2 regions. We examined the biological effects of sLRP6E1E2 binding to extracellular Wnt ligands and blocking ligand-receptor interactions. Our results provide direct evidence that specific Wnt ligand/receptor interactions have potential use as anticancer therapeutic agents.

II. MATERIAL AND METHODS

1. Ethics Statement

Animal handling was conducted in accordance with national and international guidelines, in an animal facility accredited by the Association for Assessment and Accreditation of Laboratory Animal Care (AAALAC). The number of animals used was minimized, and all necessary precautions were taken to mitigate pain or suffering. Protocols were approved by the Institutional Animal Care and Use Committee at Yonsei University Health System (2010-0160).

2. Materials

Polyclonal antibodies against MAPK kinase (MEK1/2), p44/42 mitogen-activated protein kinase (MAPK; Erk1/2), mTOR, phosphatidylinositol 3-kinase (PI3K) and Akt, and monoclonal antibodies against Wnt3a, Dvl2, Axin, glycogen synthase kinase (GSK3- β), poly (ADP-ribose) polymerase (PARP), cleaved caspase-3 and Keratin 18 (DC10) were purchased from Cell Signaling Technology (Beverly, MA). Antibodies against epithelial-to-mesenchymal transition (EMT)-related molecules β -catenin, E-cadherin and vimentin were obtained from Cell Signaling Technology, and antibody against N-cadherin was purchased from eBioscience (San Diego,

CA). Antibodies against cyclin D1 (H-295), cytochrome *c* (C-20 for Western blot analysis), and LRP6 (C-10) and protein A/G agarose beads were purchased from Santa Cruz Biotechnology (Santa Cruz, CA). Monoclonal antibody against Keratin 8 was from OriGene Technologies (Rockville, MD). Polyclonal antibody against Keratin 14 was from Anaspec (San Jose, CA). Monoclonal antibody against caspase-3 was from StressGen Biotechnologies (Victoria, BC). Polyclonal antibody against cytochrome *c* (6H2.B4 for Immunohistochemistry) was from BD Pharmingen (San Diego, CA). Snail was purchased from Abcam (Cambridge, MA). Alexa Fluor 488-conjugated and Alexa Fluor 568-conjugated anti-rabbit IgG antibodies were obtained from Invitrogen (Carlsbad, CA). DAPI (1 µg/ml), Hoechst 33342, and tetramethylrhodamine isothiocyanate (TRITC)-conjugated phalloidin were from Sigma (St. Louis, MO). Purified Wnt3a protein was purchased from R&D Systems (Minneapolis, MN).

3. Cell lines and culture conditions

Non-small cell lung cancer cell lines A549, H460, H358, and H596 were maintained in Dulbecco's modified high-glucose Eagle's medium (DMEM; Life Technologies, Grand Island, NY); H322, H2009 and H1299 cell lines were cultured in RPMI 1640 (Life Technologies, CA) medium

supplemented with 10% fetal bovine serum, 2 mM L-glutamine, 1 mM sodium pyruvate, 1% MEM nonessential amino acids, penicillin-streptomycin (100 IU/ml), and Hank's balanced salt solution (Life Technologies, CA). Cells were purchased from the American Type Culture Collection (Manassas, VA) and maintained at 37°C in a humidified chamber at 5% CO₂. Human breast cancer cell line SK-BR-3 and MDA-MB-468 were also obtained from American Type Culture Collection (ATCC) and grown per American Type Culture Collection recommendations.

4. Luciferase reporter assay for β -catenin activity

TOPflash and FOPflash luciferase reporter vectors (Upstate Biotechnology, Lake Placid, NY) were used to measure β -catenin/T-cell factor (TCF) signaling activity. Cells were seeded into 6-well plates and transfected with 0.3 μ g TOPflash (containing wild-type TCF binding sites) or FOPflash (containing mutated TCF binding sites) negative control with dE1-k35/LacZ or dE1-k35/sLRP6E1E2 (20, 50 MOI) in serum-free medium. After 12 hr, the medium was replaced with 1% DMEM with or without 100 ng/ml of Wnt3a, and the cells were incubated for another 24 hr. Cells were lysed with passive lysis buffer, and 20 μ l of the cell extract was analyzed using the Dual-

Luciferase Reporter Assay System (Promega, Madison, WI). Experiments were carried out in triplicate and repeated at least three times.

5. Cell proliferation assay

The cell proliferation assay was determined by 3-(4, 5-dimethylthiazol-2-yl)-2,5-diphenyl-tetrazolium bromide (MTT) assay (Sigma, MO). A549 and H322 cells were seeded in 24-well plates (2×10^4 cells/well). After 24 hr, cells were treated with PBS, dE1-k35/LacZ, or dE1-k35/sLRP6E1E2. The next day, cells were stimulated with or without recombinant Wnt3a (100 ng/ml) for an additional 48 hr. Absorbance at 540 nm was read on a microplate reader. All assays were performed in triplicate.

6. Western blotting

Cells cultured in DMEM with 1% fetal bovine serum in 100-mm plates were transduced with dE1-k35/LacZ or dE1-k35/sLRP6E1E2. The next day, cells were treated with or without Wnt3a (100 ng/ml) for 16 hr. Immunoblotting was performed as described previously¹⁶. Blocked membranes were examined using target gene specific primary antibody overnight at 4°C. The blots were incubated with the following secondary antibodies conjugated to horseradish peroxidase: goat anti-rabbit IgG, goat

anti-mouse IgG, or mouse anti-goat IgG (Cell Signaling Technology) and developed using enhanced chemiluminescence (Amersham Pharmacia Biotech, Uppsala, Sweden).

7. Immunofluorescence assay

For immunofluorescence microscopy, cultured cells were washed twice with PBS, fixed in 4% paraformaldehyde for 10 min at room temperature, and then permeabilized by incubation for 15 min with 0.1% Triton X-100 in PBS. The samples were blocked with 1% bovine serum albumin followed by incubation with E-cadherin, β -catenin, or anti-cytochrome *c* primary antibodies overnight at 4°C. The next day, cells were washed with PBS and incubated with Alexa Fluor 488-conjugated goat anti-rabbit IgG secondary antibody for 60 min at room temperature. The final antibody treatment also contained TRITC-conjugated actin and Hoechst 33342 or DAPI stain (both at 1 μ g/ml, Sigma) for nuclear staining. Slides were mounted with Vectashield mounting medium (Vector Laboratories, Burlingame, CA), and cells were viewed under a confocal laser-scanning microscope (LSM510, Carl Zeiss MicroImaging, Thornwood, NY).

8. Mitochondrial fractionation and western blotting

Mitochondrial fractions were prepared using the Qproteome mitochondria isolation kit (QIAGEN, Hilden, Germany) following the manufacturer's instructions. Cells washed with 0.9% sodium chloride solution were suspended with ice-cold lysis buffer by pipetting up and down. After a 10-min incubation, lysate was centrifuged at 1000 g for 10 min at 4°C, and the supernatant containing cytosolic proteins was carefully removed. The pellet containing nuclei, cell debris, and unbroken cells was resuspended with ice-cold disruption buffer and centrifuged at 1000 g for 10 min at 4°C, and the supernatant (microsomal fraction) was transferred to a clean microtube. The resulting pellet containing mitochondria was washed with the mitochondria storage buffer and centrifuged at 6000 g for 20 min at 4°C; a band toward the bottom of the tube was harvested as a mitochondrial fraction. Western blotting was performed with the rabbit anti-cytochrome *c* antibody using the procedure described above.

9. Anti-tumor effects in xenograft model

Human non-small cell lung cancer (H460) and human breast cancer (SKBR3) xenograft were established in 6- to 8-week-old male athymic nu/nu mice (Charles River Japan, Yokohama, Japan) by subcutaneous implantation of 1×10^7 H460 and SKBR3 cells in the abdomen. When tumor volumes

reached approximately 80-100 mm³, the mice were divided experiment groups with similar mean tumor volumes. In H460 cells, adenoviral vectors were administered intratumorally (2×10^{10} viral particles/mouse) on the first day of treatment (day 1) and days 3 and 5. In SKBR3 cells, adenoviral vectors were administered intratumorally (5×10^{10} viral particles/mouse) on the first day of treatment (day 1) and days 3, 5, 7 and 9. All animal studies were conducted in the Yonsei University College of Medicine according to institutional regulations, in an animal facility accredited by the Association for Assessment and Accreditation of Laboratory Animal Care (AAALAC). Tumor volume (V) was calculated as $V = 0.52 \times a^2 \times b$ (a , smallest superficial diameter; b , largest superficial diameter).

10. Tumor histology and immunohistochemistry

Tumor tissue was fixed in 4% paraformaldehyde and embedded in paraffin wax for histologic examination and immunohistochemical staining. Representative sections were stained with hematoxylin and eosin and examined by light microscopy. To quantify capillary density and Wnt expression, the tumor sections were stained with anti-mouse CD31 IgG (BD Pharmingen), anti-rabbit β -catenin IgG (Cell Signaling Technology), or anti-mouse Wnt3a IgG (Santa Cruz Biotechnology). The breast tumor samples

were stained with antibodies recognizing PCNA. After quenching endogenous peroxidase activity and blocking non-specific protein binding with normal goat serum (Vector Laboratories), sections were incubated with primary antibodies at 4°C overnight, and then with biotinylated secondary IgG (Jackson ImmunoResearch, West Grove, PA). Positive immunoreactivity was visualized with ABC-peroxidase kits (ChemMate™ DAKO Envision™ Detection kit; DAKO). Controls were prepared by incubating with irrelevant class-matched and species-matched IgGs. All slides were counterstained with Mayer's hematoxylin. The expression levels of Wnt3a and β -catenin were assessed semi-quantitatively using MetaMorph® image analysis software (Universal Image Corp., Westchester, PA). Results were expressed as mean optical density for five different digital images.

11. Terminal deoxynucleotidyl transferase dUTP nick end labeling assay

The 5- μ m formalin-fixed and paraffin-embedded tissue sections were deparaffinized and rehydrated according to standard protocols¹⁷. Apoptosis was detected with the terminal deoxynucleotidyl transferase dUTP nick end labeling (TUNEL) assay (DeadEnd™ Fluorometric TUNEL System; Promega). Briefly, tissue sections were permeabilized with proteinase K (20 μ g/ml) for 10 min at room temperature. Sections were then incubated with

terminal deoxynucleotidyl transferase (TdT) and fluorescein-12-dUTP in TdT buffer at room temperature for 60 min and washed with TdT buffer. Finally, nuclei were counterstained with DAPI. The samples were analyzed by fluorescence microscopy using a standard fluorescent filter.

12. Migration and invasion assay

In vitro migration assays were performed as described previously¹⁸. Briefly, the lower surface of 6.5-mm polycarbonate filters (8- μ m pore size; Corning Costar, Cambridge, MA) was coated by immersion in 0.1% gelatin. Conditioned media was obtained from A549, SKBR3 and MDA-MB-468 cells transduced with PBS, dE1-k35/LacZ and dE1-k35/sLRP6E1E2 after treatment with or without Wnt3a and placed in the bottom Transwell chamber. Cells were then plated on the upper chamber (7×10^4 cells/well). Cultures were incubated at 37°C for 4 hr, fixed, and stained with hematoxylin and eosin. *In vitro* Matrigel invasion assays were performed using bio-coat cell migration chambers. Filters (8- μ m pore) were coated with Matrigel basement membrane matrix (37 mg/filter; BD Biosciences, San Jose, CA), and the experiment was performed as described for the cell migration assay. After 24 hr, noninvading cells were removed, and the invading cells on the under surface of the filter were fixed and stained. The membranes were mounted on glass slides, and

migrated cells were counted at 200× magnification. Five fields were counted for each assay, and experiments were repeated at least three times.

13. Statistical analysis

Results are expressed as mean \pm standard error of the mean (SEM). Group results were compared by one-way analysis of variance, followed by post hoc Student's *t*-test for unpaired observations or Bonferroni's correction for multiple comparisons when appropriate. $P < 0.05$ was considered significant.

III. RESULTS

1. Generation of adenoviral vectors expressing soluble LRP6 receptor

To study the biochemical function of soluble LRP6 receptor (sLRP6E1E2), we generated constructs of the E1 and E2 extracellular domains (Wnt-binding sites) of LRP6¹⁹ and FLAG-tagged sLRP6E1E2 cDNA fragment was subcloned into a pCA14 shuttle vector²⁰. This pCA14-sLRP6E1E2 vector was co-transformed with a replication-incompetent adenovirus 5/35 chimeric vector (dE1-k35) or replication-competent chimeric oncolytic adenovirus vector (RdB-k35)¹⁶, generating pdE1-k35/sLRP6E1E2 and pRdB-k35/sLRP6E1E2, respectively. The replication-incompetent dE1-k35/LacZ and replication-competent oncolytic RdB-k35 vectors were used as negative controls²¹ (Fig. 1).

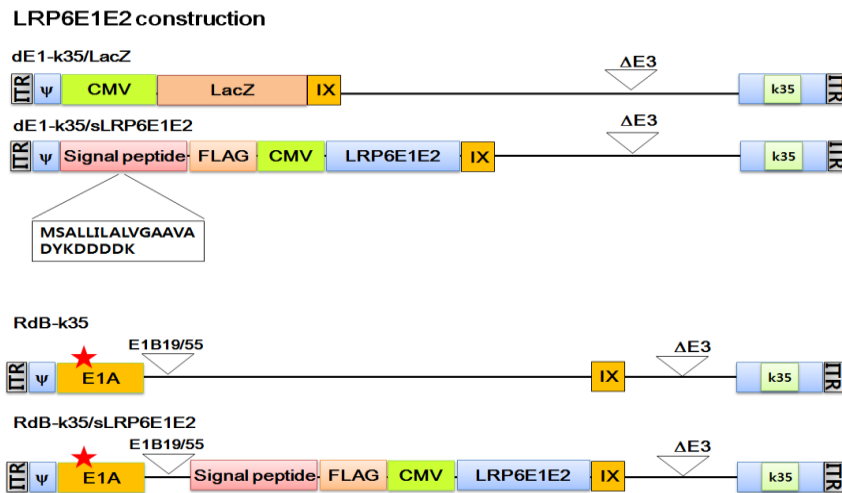


Figure 1. Constructs of the adenoviral (Ad) vectors (a) E1-deleted replication-incompetent Ads. dE1-k35 expresses β -galactosidase under the control of the cytomegalovirus (CMV) promoter, dE1-k35/LRP6E1E2 expresses LRP6E1E2 in the E1 region. (B) Oncolytic Ads. RdB contains mutated E1A, but lacks E1B 19 and 55kDa; RdB/LRP6E1E2 expresses LRP6E1E2 in the E1 region.

2. Soluble Wnt decoy receptor is expressed in lung cancer cell lines

Endogenous Wnt3a and LRP6 levels were assessed in seven non-small cell lung cancer cell lines (A549, H322, H596, H460, H358, and H2009) by western blot analysis. Both Wnt3a and LRP6 were more strongly expressed in H322, H460, and H2009 cells than in other cell lines (Fig. 2A); therefore, H322 and H460 cells were selected to evaluate the ability of the soluble Wnt decoy receptor (sLRP6E1E2) to inhibit Wnt signaling. Expression of sLRP6E1E2 from dE1-k35/sLRP6E1E2-transduced A549 cells was confirmed by western blot analysis using anti-FLAG antibodies (Fig. 2B). Secretion of sLRP6E1E2 from dE-k35/sLRP6E1E2-transduced cells was dose-dependent. To ensure equal loading, transferred proteins were visualized by staining with Ponceau Red.

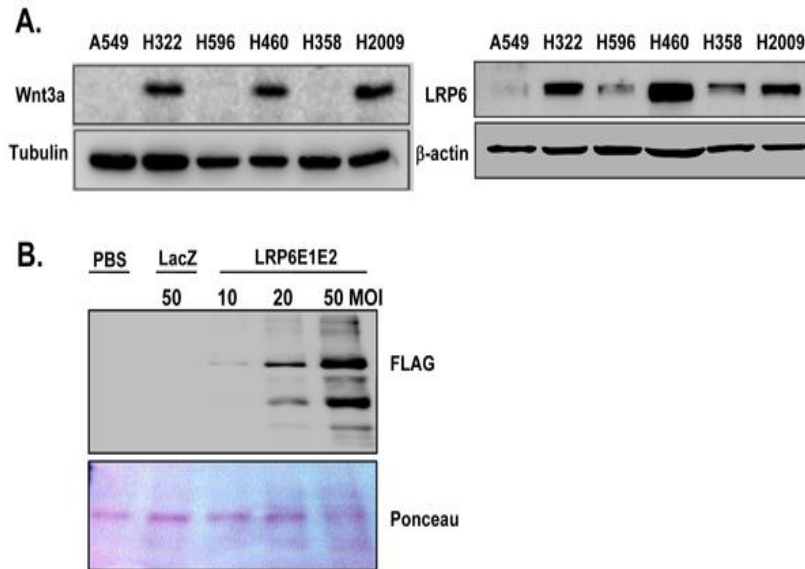


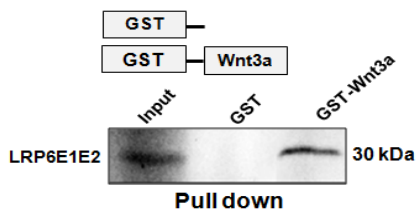
Figure 2. Characterization of the decoy Wnt receptor sLRP6E1E2 (a) Endogenous Wnt3a (left panel) and LRP6 (right panel) expression in several human lung cancer cell lines. (b) Secretion and expression of sLRP6E1E2. Supernatants of cell culture were assessed with FLAG specific Ab (Upper panel). Ponceau staining is to demonstrate equal amount of sLRP6E1E2 loading (Bottom panel).

3. Soluble Wnt decoy receptor binds to Wnt3a

Next, binding of sLRP6E1E2 to Wnt3a was assessed by GST pull-down assay. As shown in Fig. 3A, GST-Wnt3a fusion protein interacted with

LRP6E1E2 protein *in vitro*, suggesting that sLRP6E1E2 can bind to Wnt3a directly. We then investigated if soluble LRP6E1E2 expressed from dE1-k35/sLRP6E1E2 can interfere the binding ability of endogenous LRP6 to Wnt3a. Cell lysates of dE1-k35/LacZ- or dE1-k35/sLRP6E1E2-transduced H322 and H460 cells which endogenously overexpress Wnt3a were immunoprecipitated with Wnt3a or LRP6 antibody, and then endogenous Wnt3a (top) and total LRP6 (bottom) levels were detected with anti-Wnt3a and anti-LRP6 antibody. We observed that both Wnt3a and LRP6 protein levels were lower in cells transduced with dE1-k35/sLRP6E1E2 than in cells transduced with dE1-k35/LacZ (Fig. 3B), demonstrating that exogenously expressed sLRP6E1E2 can efficiently bind to Wnt3a, leading to prevention of the interaction between endogenous LRP6 and Wnt3a.

A.



B.

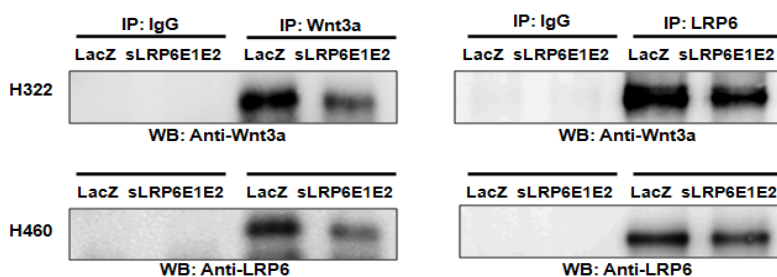
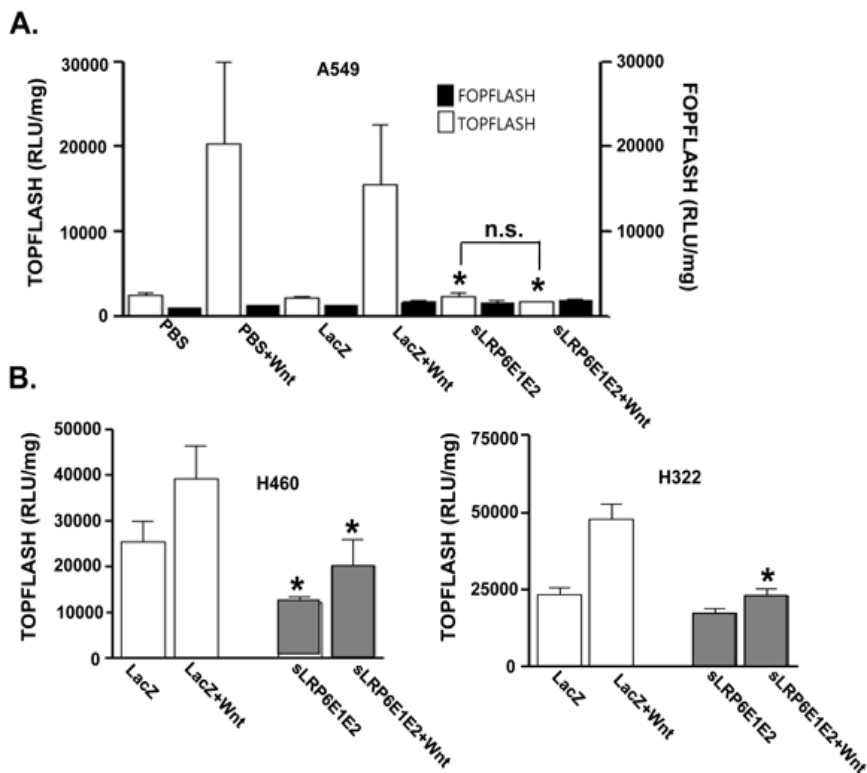


Figure 3. Soluble Wnt decoy receptor binds to Wnt3a. (a) GST fusion protein pull-down assay. Recombinant GST and GST-Wnt3a protein was incubated with [³⁵S]methionine-labeled LRP6E1E2, pulled down, and resolved by a 12-15% SDS-PAGE. (b) H322 and H460 cells were transduced with dE1-k35/LacZ or dE1-k35/sLRP6E1E2 (50 MOI) for 48 hr. Cell lysates were immunoprecipitated with antisera against Wnt3a (IP: Wnt3a) or LRP6 (IP: LRP6) followed by western blot analysis with the same antibodies.

4. Decoy Wnt receptor decreases cytosolic β -catenin level and TCF transcriptional activity

We next hypothesized that secreted sLRP6E1E2 protein inhibits Wnt signaling by direct binding to Wnt. Therefore, to characterize the sLRP6E1E2 effects on the Wnt3a/ β -catenin signaling, we determined its effect on β -catenin using a luciferase reporter system activated by β -catenin/TCF²². As shown in Fig. 4A, luciferase activity was low in A549 cells transduced with dE1-k35/LacZ or dE1-k35/sLRP6E1E2 in the absence of Wnt3a, since the endogenous expression level of Wnt3a in A549 is very minimal (Fig. 4A). Wnt3a treatment increased luciferase expression approximately 7- to 8-fold in control cells, but not in dE1-k35/sLRP6E1E2-transduced cells, suggesting that secreted sLRP6E1E2 could block the

signaling effect of exogenously treated Wnt3a. In the absence of Wnt3a, luciferase activity was reduced by dE1-k35/sLRP6E1E2 in H460 (48%) and H322 (12%) cells compared with dE1-k35/LacZ controls (Fig. 4B; $P < 0.05$). Wnt3a stimulation increased luciferase activity in H460 (53%) and H322 (102%) cells transduced with dE1-k35/LacZ, but luciferase activity was significantly lower in dE1-k35/sLRP6E1E2-transduced H460 (48%) and H322 (52%) cells compared with dE1-k35/LacZ ($P < 0.05$).



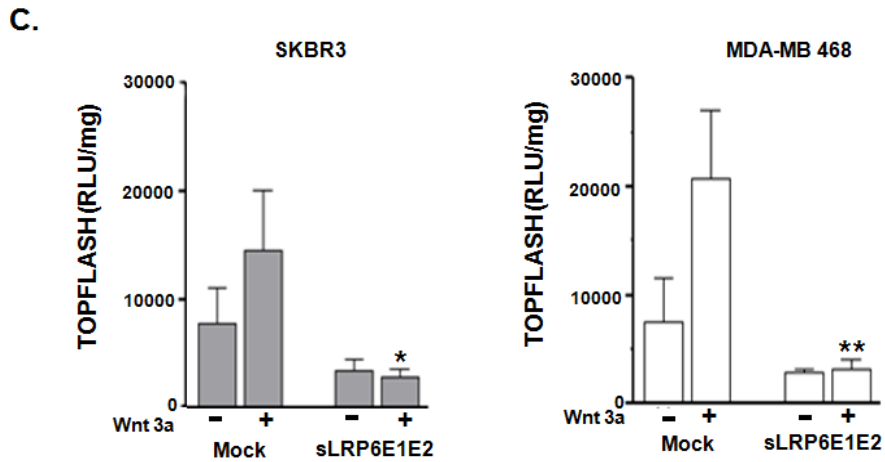


Figure 4. Decoy Wnt receptor sLRP6E1E2 reduces T-cell factor transcriptional activity. (a) TCF/LEF luciferase reporter assay in A549 cells. To characterize the sLRP6E1E2 effects on the Wnt3a/ β -catenin signaling, cells were transfected with TOPflash (containing wild-type TCF binding sites) or FOPflash (containing mutated TCF binding sites) luciferase vector. * $P < 0.05$ versus dE1-k35/LacZ-transduced or PBS-treated cells. (b) TCF/LEF luciferase reporter assay in lung cancer cells. * $P < 0.05$ versus PBS or dE1-k35/LacZ-transduced cells with or without Wnt3a. (c) TCF/LEF luciferase reporter assay in breast cancer cells. * $P < 0.05$, ** $P < 0.01$ versus dE1-k35/Mock transduced cells with Wnt3a.

Next we also confirmed the β -catenin transcriptional activity in breast cancer cell lines. In the absence of Wnt3a, luciferase activity was reduced by dE1-

k35/sLRP6E1E2 in SKBR3 (56.71 %) and MDA-MB-468 (62.61 %) cells compared with dE1-k35/Mock. Wnt3a stimulation increased luciferase activity in SKBR3 (84.98 %) and MDA-MB-468 (176.79 %) cells transduced with dE1-k35/Mock, but luciferase activity was significantly lower in dE1-k35/sLRP6E1E2-transduced SKBR3 (80.17 %) and MDA-MB-468 (84.65 %) cells compared with dE1-k35/Mock (Fig 4C). These results suggest that sLRP6E1E2 can be sufficient to block Wnt signaling in different cancer cells.

To evaluate the effect of sLRP6E1E2 on β -catenin localization, immunofluorescence staining was performed in H322 cells treated with PBS or transduced with dE1-k35/LacZ or dE1-k35/sLRP6E1E2. In the absence of Wnt3a, β -catenin staining was restricted primarily to cell–cell contact sites in all groups. Upon Wnt3a stimulation, control cells (PBS and dE1-k35/LacZ) showed reduced β -catenin localization at the plasma membrane, especially at cell–cell junctions, and increased β -catenin levels in the cytosol and nucleus. In contrast, dE1-k35/sLRP6E1E2-transduced cells showed lower levels of cytosolic β -catenin, and higher levels of membrane-associated β -catenin (Fig. 5A). Quantification of the nucleus β -catenin expression showed a 98.08% decrease in dE1-k35/sLRP6E1E2-transduced cells compared with dE1-k35/LacZ controls in the presence of Wnt3a (Fig. 5B). Results of these functional studies demonstrate that interactions between sLRP6E1E2 and Wnt

may be sufficient to block Wnt signaling

As a similar result, upon Wnt3a stimulation, SK-BR-3 and MDA-MB-468 cells (PBS and dE1-k35/Mock) showed reduced β -catenin localization at the plasma membrane and increased β -catenin levels in the cytosol and nucleus. In contrast, sLRP6E1E2-transduced cells showed predominantly in the plasma membrane with weekly levels of cytoplasmic and nuclear staining (Fig 5C and D).

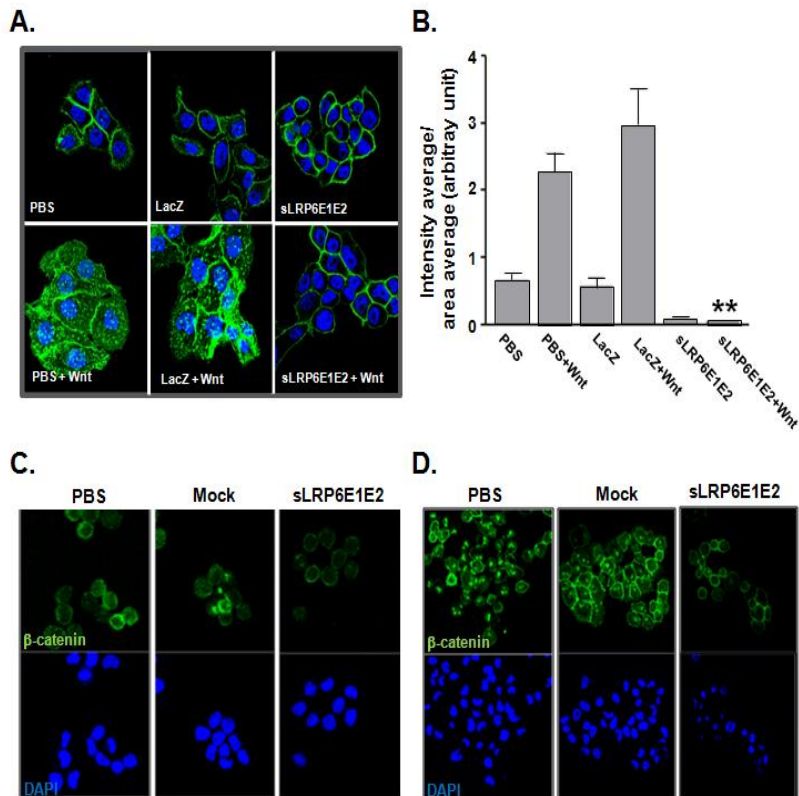


Figure 5. Effect of Decoy Wnt receptor sLRP6E1E2 on β -catenin localization (a) H322 cells were transduced with dE1-k35/LacZ or dE1-k35/sLRP6E1E2 (50 MOI) with or without Wnt3a. Cells were labeled with anti- β -catenin. Original magnification, $\times 630$. (b) Semi-quantitative analysis of panel (a) results using MetaMorph® imaging analysis software. Each data point indicates mean \pm SEM (each group, n=5). ** $P < 0.001$ versus PBS or dE1-k35/LacZ-transduced cells with Wnt3a. (c) SKBR3 and (d) MDA-MB-468 cells were transduced with dE1-k35/Mock or dE1-k35/sLRP6E1E2 (50 MOI). Cells were labeled with anti- β -catenin. Original magnification, $\times 630$

5. Decoy Wnt receptor sLRP6E1E2 inhibits lung cancer cell proliferation

The Wnt pathway regulates a wide range of cellular functions including proliferation²³. To test the effects of sLRP6E1E2 on proliferation of A549 and H322 cells *in vitro*, cells were treated with PBS or transduced with dE1-k35/LacZ or dE1-k35/sLRP6E1E2. At 72 hr after transduction with dE1-k35/sLRP6E1E2 (20 MOI), cell proliferation was reduced by 39% in A549 cells and 51% in H322 cells compared with dE1-k35/LacZ-transduced controls. Wnt3a stimulation increased proliferation approximately 10-20% in control cells, but had no apparent effect on dE1-k35/sLRP6E1E2-transduced cells. Proliferation was 54% lower in A549 cells and 61% lower in H322 dE1-

k35/sLRP6E1E2-transduced cells than dE1-k35/LacZ-transduced cells ($P<0.001$; Fig. 6A and 6B).

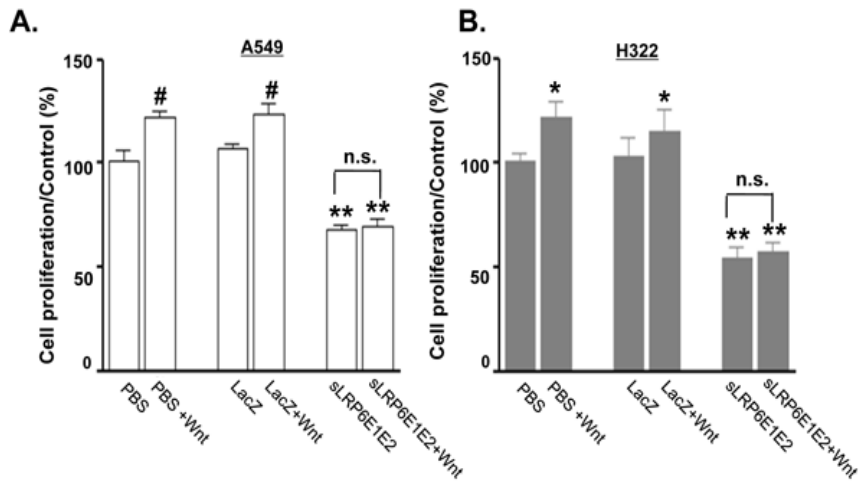


Figure 6. Decoy Wnt receptor sLRP6E1E2 decreases proliferation in human lung cancer cells. (a) A549 and (b) H322 cells were transduced with dE1-k35/LacZ or dE1-k35/sLRP6E1E2 (20 MOI). The next day, these cells were incubated with or without Wnt3a (100 ng/ml). After 3 days, cell proliferation was assessed by the MTT assay (mean \pm SEM). * $P<0.05$, # $P<0.01$ versus untreated control for each group; ** $P<0.001$ versus dE1-k35/LacZ-transduced or PBS-treated cells. n.s. = not significant.

6. Decoy Wnt receptor sLRP6E1E2 down-regulated both the Wnt and ERK, PI3K pathways

To characterize signaling pathways involved in the anti-proliferative action of sLRP6E1E2, we examined its effects on canonical Wnt signaling. As shown in Fig. 7A, LRP6, Dvl2 and Axin protein levels in control cells (PBS and dE1-k35/LacZ) were increased by Wnt3a, but were apparently unaltered by Wnt3a in dE1-k35/sLRP6E1E2-transduced cells. Similarly, cyclin D1 expression was slightly increased in control cells following Wnt3a stimulation, but slightly decreased in dE1-k35/sLRP6E1E2-transduced cells. GSK3 β levels also appeared slightly decreased after Wnt3a treatment.

Wnt plays a fundamental role in proliferation by activating Erk1/2 and PI3K-Akt pathways²⁴. We therefore investigated whether sLRP6E1E2 can downregulate these pathways. As shown in Fig. 7B, phosphorylation of Erk1/2, PI3K, and Akt was upregulated by Wnt3a treatment, but levels of phosphorylation was lower in dE1-k35/sLRP6E1E2-transduced cells compared to those in PBS-treated and dE1-k35/LacZ-transduced cells. Expression of mTOR, PI3K, and Akt was not affected by Wnt3a stimulation, and was lower in dE1-k35/sLRP6E1E2-transduced cells than controls in H460 cells. Taken together, these results suggest that sLRP6E1E2 exerts antiproliferative actions by inhibiting Wnt signaling via MEK-ERK and

PI3K- Akt pathways.

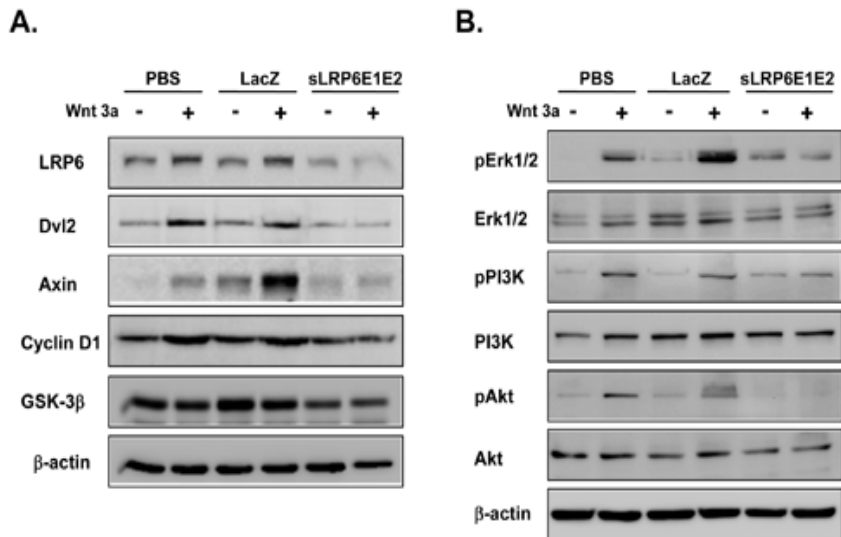


Figure 7. Decoy Wnt receptor sLRP6E1E2 decreases Wnt signaling and MEK-ERK and PI3K- Akt signaling (a) A549 cells were treated as indicated above (Fig. 6a). Western blot using antibodies specific to LRP6, Dvl2, Axin, Cyclin D1, or GSK-3β. (b) A549 cells were harvested at 6 hr after Wnt3a treatment. The p-Erk1/2, Erk1/2, p-PI3K, PI3K, p-Akt, and Akt proteins were detected by western blot analysis.

7. Decoy Wnt receptor sLRP6E1E2 induces apoptosis

Wnt signaling can prevent apoptosis and promote cellular proliferation and survival²⁵. To characterize the molecular mechanisms by

which sLRP6E1E2 inhibits non-small cell lung cancer proliferation, we evaluated the effects of sLRP6E1E2 on apoptosis. At 3 days after dE1-k35/sLRP6E1E2 transduction, we observed that A549, H1299, and H358 cells gradually detached from the culture dish and became rounder and smaller than attached cells (data not shown), suggesting that sLRP6E1E2 induced apoptosis. Evidence of apoptosis was sought by looking for nuclear apoptotic bodies, and then assessed using the TUNEL assay to detect internucleosomal DNA fragmentation ²⁶. As shown in Fig. 8A, more TUNEL-positive cells were observed among dE1-k35/sLRP6E1E2-transduced cells than among control cells in the presence or absence of Wnt3a. Quantitation of TUNEL staining revealed that the rate of apoptosis was approximately 1.9-fold higher (without Wnt3a) and 2.8-fold higher (with Wnt3a) in dE1-k35/sLRP6E1E2-transduced cells than in dE1-k35/LacZ-transduced controls ($P<0.001$) (Fig. 8B).

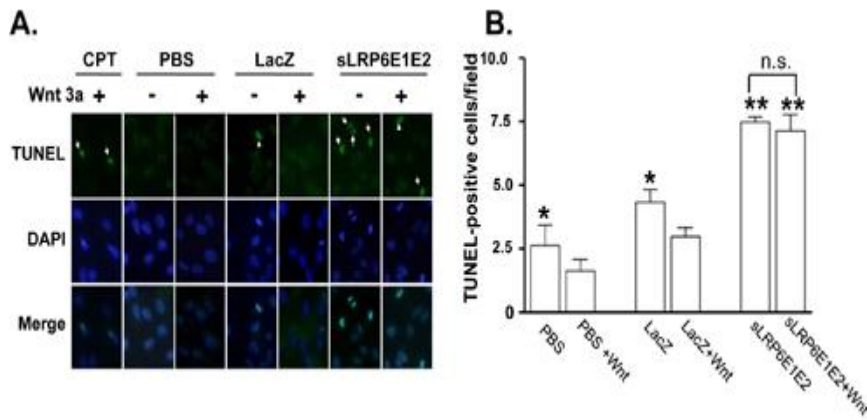
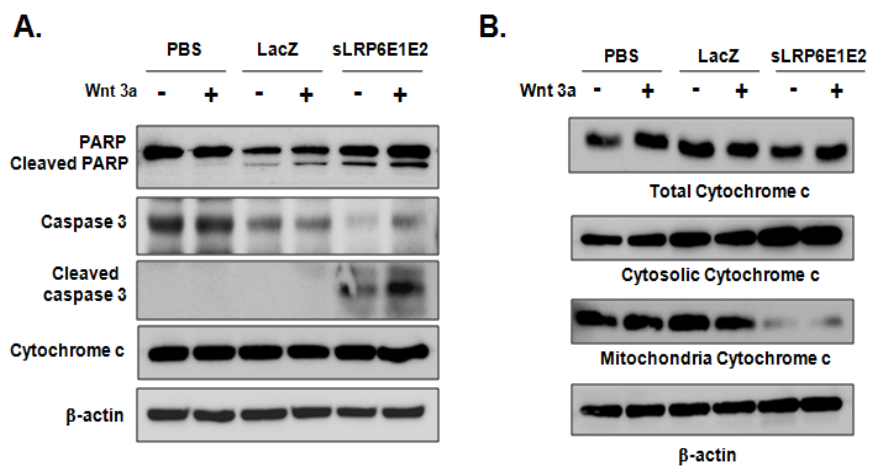


Figure 8. Decoy Wnt receptor sLRP6E1E2 induces apoptosis in human lung cancer cells. (a) Detection of sLRP6E1E2-induced apoptosis by TUNEL staining. Original magnification, $\times 400$. (b) Total number of TUNEL-positive cells per fields (mean \pm SEM). * $P < 0.05$ versus PBS or dE1-k35/LacZ treated with Wnt3a; ** $P < 0.001$ versus PBS-treated or dE1-k35/LacZ-transduced controls. n.s. = not significant.

8. Decoy Wnt receptor sLRP6E1E2 increased cytochrome c-dependent caspase activation

We next evaluated regulators of apoptosis, of which the caspase family and cytochrome *c* are the best characterized. In the absence and presence of Wnt3a, full-length 116-kDa PARP protein was reduced and 85-

kDa cleavage fragments were increased in dE1-k35/sLRP6E1E2-transduced cells (Fig. 9A). Levels of the cleaved (active) form of caspase-3 were also markedly increased by sLRP6E1E2. As shown in Fig. 9B, dE1-k35/sLRP6E1E2-transduced cells also showed increased cytosolic cytochrome *c* and decreased microsomal cytochrome *c*. Stimulation with Wnt3a produced similar effects. To further investigate cytochrome *c* localization, immunofluorescence was performed. PBS-treated and dE1-k35/LacZ-transduced cells displayed punctuate cytoplasmic staining of cytochrome *c*, consistent with mitochondrial localization. In contrast, cells expressing sLRP6E1E2 exhibited mostly diffuse cytoplasmic cytochrome *c* staining, consistent with translocation from mitochondria to cytoplasm (Fig. 9C).



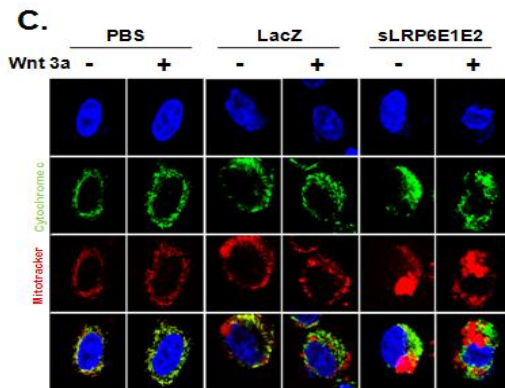


Figure 9. Decoy Wnt receptor sLRP6E1E2 regulate the release of apoptogenic cytochrome c (a) Western analysis of sLRP6E1E2-mediated apoptosis. H460 cells were transduced with dE1-k35/LacZ or dE1-k35/sLRP6E1E2 (20 MOI). The western blot using specific antibodies against uncleaved PARP, cleaved PARP, pro-caspase-3, cleaved caspase-3, and cytochrome *c*. (b) H460 cells were treated as indicated above (Fig. 8b). Subcellular localization of cytochrome *c* was determined by western blot analysis of cytosolic and microsomal fractions. (c) A549 cells were treated as indicated above (Fig. 4d). Cells were stained with anti-cytochrome *c* (green) and MitoTracker (red) and examined by laser fluorescence confocal microscopy. Original magnification, $\times 1260$.

9. Decoy Wnt receptor sLRP6E1E2 inhibits lung tumor xenograft growth

We next evaluated the ability of sLRP6E1E2 to inhibit lung tumor growth in a mouse xenograft model. Tumors were generated by subcutaneous injection of H460 cells into the abdominal region of nude mice. When tumors reached a mean size of 80-100 mm³, they were injected with PBS, dE1-k35, RdB-k35, dE1-k35/sLRP6E1E2, or RdB-k35/sLRP6E1E2 on days 1, 3, and 5. Fig. 10A shows that the volume of tumors injected with sLRP6E1E2-expressing vectors was significantly lower than that of corresponding controls. After 25 days, tumors treated with PBS reached a mean volume of 3883.1±418.08 mm³, and tumors treated with dE1-k35 and RdB-k35 reached 3388.1±226.9 mm³ and 1991±311.8 mm³, respectively. In contrast, tumor growth was strongly suppressed in mice injected with dE1-k35/sLRP6E1E2 (1645.3±353.6 mm³; $P < 0.05$ compared with PBS or dE1-k35 groups) or RdB-k35/sLRP6E1E2 (923.3±180.4 mm³; $P < 0.01$ compared with PBS or RdB-k35 groups).

To evaluate the biological effects of sLRP6E1E2 in tumor tissue, tumors were harvested 3 days after the final adenovirus injection. Analysis of adenoviral E1A protein expression revealed that RdB-k35 and RdB-k35/sLRP6E1E2 had replicated and spread through the tumor (Fig. 10B, E1A). Immunohistochemical analysis of sLRP6E1E2 (Fig. 10B, FLAG) showed that

its expression was more widespread in RdB-k35/sLRP6E1E2-treated tumors than in dE1-k35/sLRP6E1E2-treated tumors, indicating that the oncolytic adenovirus more efficiently expressed sLRP6E1E2 than the replication-incompetent adenovirus, contributing to its superior antitumor actions.

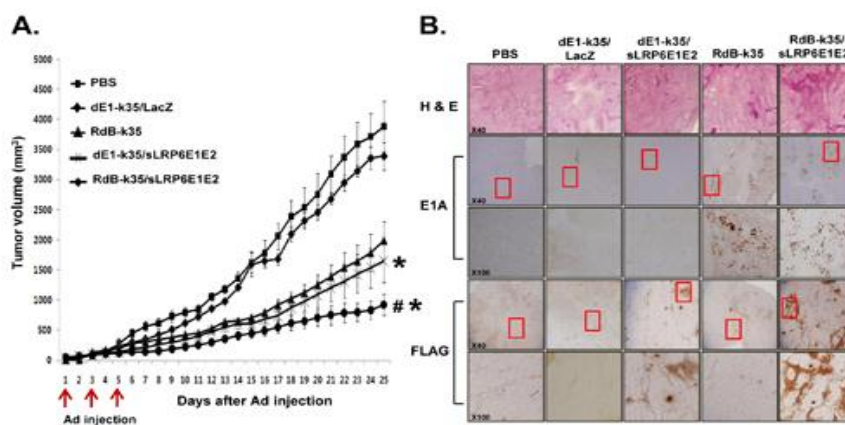


Figure 10. Decoy Wnt receptor sLRP6E1E2 inhibit *in vivo* tumor growth
 (a) Tumors were injected with PBS (■), dE1-k35/LacZ (◆), RdB-k35 (▲), dE1-k35/sLRP6E1E2 (×), or RdB-k35/sLRP6E1E2 (●) on days 1, 3, and 5. Results are expressed as mean \pm SEM (n=7). * P <0.05 versus PBS-treated or dE1-k35-treated controls and versus dE1-k35/sLRP6E1E2. # P <0.01 versus PBS-treated or dE1-k35-treated controls. (b) Tumor sections from each group were immunostained against E1A or FLAG (original magnification, $\times 40$ and $\times 100$).

10. Anti-proliferative and apoptotic effects of sLRP6E1E2-expressing vectors in H460 xenografts

To assess the effects of sLRP6E1E2 on tumor xenograft growth in mice, tumor samples were analyzed by Ki-67 immunostaining for proliferating cells and TUNEL staining for apoptotic cells. We found that Ki-67 expression was reduced and TUNEL-positive cells were increased in tumors treated with dE1-k35/sLRP6E1E2 or RdB-k35/sLRP6E1E2 compared with corresponding controls (Fig. 11A). We also detected more TUNEL-positive cells in RdB-k35/sLRP6E1E2-treated tumors than in dE1-k35/sLRP6E1E2-treated tumors, consistent with previous results. To determine whether the smaller sLRP6E1E2-treated tumors exhibited reduced neovascularization, microvessel density was assessed by CD31 staining. Fewer endothelial cells and vessel structures was observed in tissues injected with E1-expressing oncolytic adenoviruses (RdB-k35 and RdB-k35/sLRP6E1E2) than PBS-treated tumors ($P<0.05$), whereas no significant decrease in vascular density was observed in tumors injected with dE1-k35 or dE1-k35/sLRP6E1E2 (Fig. 11B & 11C). Further, vessel density in tumors injected with sLRP6E1E2-expressing adenoviruses did not differ from their corresponding controls, suggesting that the antitumor properties of sLRP6E1E2 were not mediated by anti-angiogenic effects.

To further investigate the role of Wnt signaling in the antitumor actions of sLRP6E1E2-expressing adenoviruses, Wnt and β -catenin localization in tumor tissue was evaluated. High endogenous expression of β -catenin and Wnt was observed in tumor tissues treated with PBS or control vectors (dE1-k35 and RdB-k35) (Fig. 11 D-F), but was significantly reduced by sLRP6E1E2-expressing vectors, suggesting that blockade of Wnt signaling in tumor cells was an important contributor to slower tumor growth.

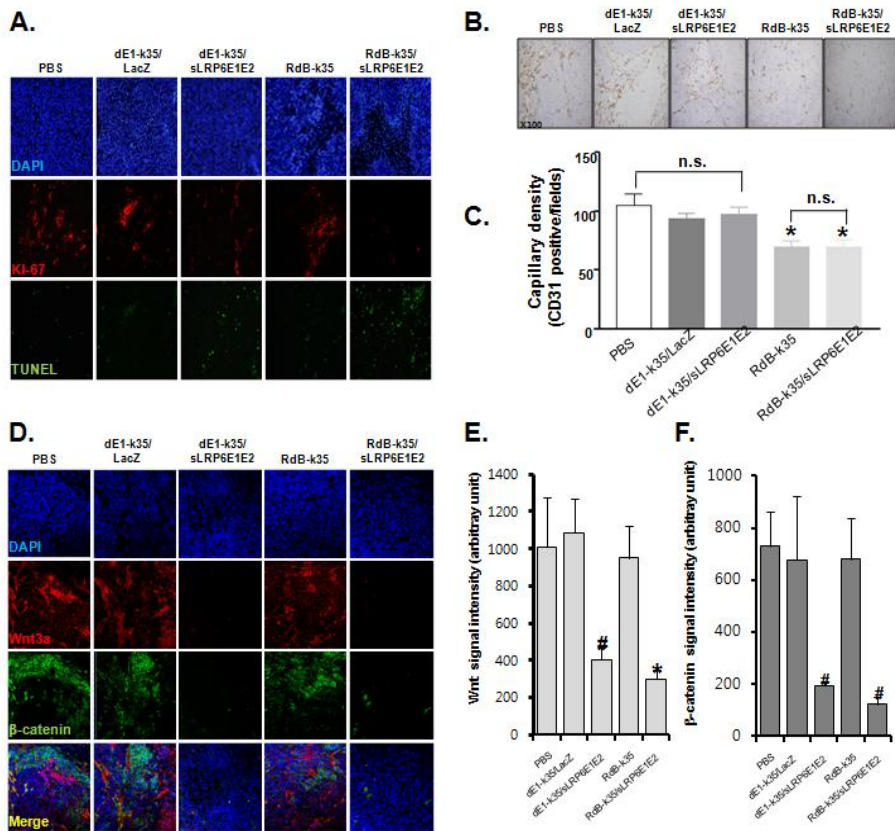


Figure 11. Histological characterization of tumor tissue in H460 xenografts (a) Tumor tissues from each group were stained with DAPI (blue), anti-Ki67 (red), and TdT-mediated TUNEL (green). Original magnification: $\times 100$. (b) Blood vessels were visualized by staining for CD31. Original magnification, $\times 100$. (c) Mean microvessel density for each treatment group (CD31 positive cells/field). Results are expressed as mean \pm SEM (each group, n=3 tumors). * $P < 0.05$ versus PBS, dE1-k35, or dE1-k35/sLRP6E1E2. n.s. = not significant. (d) Cells were stained with DAPI (blue), anti-Wnt3a (red), or anti- β -catenin (green). Original magnification: $\times 100$. (e, f) The expression levels of Wnt3a (e) and β -catenin (f) were assessed semi-quantitatively using MetaMorph® imaging analysis software. Results are expressed as mean \pm SEM (each group, n=5 tumors). # $P < 0.01$ versus dE1-k35, * $P < 0.05$ versus RdB-k35.

11. Decoy Wnt receptor sLRP6E1E2 inhibits breast tumor xenograft growth

We also tested whether LRP6E1E2 could inhibit breast tumor growth *in vivo*. Tumors were generated by subcutaneous injection of SKBR3 cells into the abdominal region of nude mice. When tumors reached a mean size of 80-100 mm³, they were injected with PBS, dE1-k35/Mock and dE1-k35/sLRP6E1E2 on days 1, 3, 5, 7 and 9. Fig. 12 shows that the volume of

tumors injected with sLRP6E1E2-expressing vectors was lower than that of corresponding controls. After 45 days, tumors treated with PBS reached a mean volume of $4463.556 \pm 462.196 \text{ mm}^3$, and tumors treated with dE1-k35/Mock reached $4304.45 \pm 249.97 \text{ mm}^3$. In contrast, tumor growth was suppressed in mice injected with dE1-k35/sLRP6E1E2 ($2442.403 \pm 376.92 \text{ mm}^3$; $P < 0.05$ compared with PBS or dE1-k35/Mock groups).

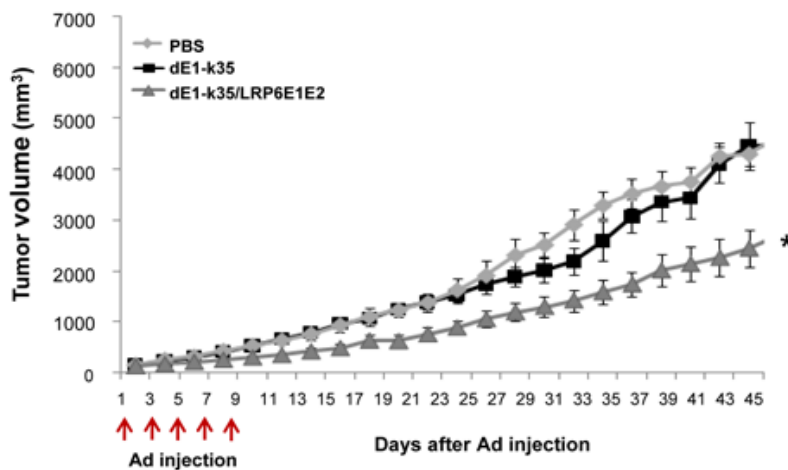


Figure 12. Anti-tumor effects of decoy Wnt receptor sLRP6E1E2 (a)

Tumors were injected with PBS (■), dE1-k35/Mock (◆), and dE1-k35/sLRP6E1E2 (×) on days 1, 3, 5, 7 and 9. Results are expressed as mean \pm SEM (n=6). * $P < 0.05$ versus PBS- or dE1-k35/Mock-treated controls and versus dE1-k35/sLRP6E1E2. # $P < 0.01$ versus PBS- or dE1-k35/Mock-treated

controls.

12. Decoy Wnt receptor sLRP6E1E2 decrease stem cell property of mice bearing breast xenografts

To evaluate the biological effects of sLRP6E1E2 on breast tumor xenograft growth in mice, tumor samples were analyzed by PCNA immunostaining for proliferating cells and vimentin staining for mesenchymal cells. We found that PCNA and vimentin expression were reduced in tumors treated with dE1-k35/sLRP6E1E2 compared with corresponding controls (Fig. 13A). To further investigate the role of Wnt signaling in the antitumor actions of sLRP6E1E2-expressing adenoviruses, Wnt and β -catenin localization in tumor tissue was evaluated expressing adenoviruses, Wnt and β -catenin localization in tumor tissue was evaluated. High endogenous expression of β -catenin and Wnt was observed in tumor tissues treated with PBS or control vectors (dE1-k35/Mock) (Fig. 13B), but was significantly reduced by sLRP6E1E2-expressing vectors, suggesting that blockade of Wnt signaling in tumor cells was an important contributor to slower tumor growth

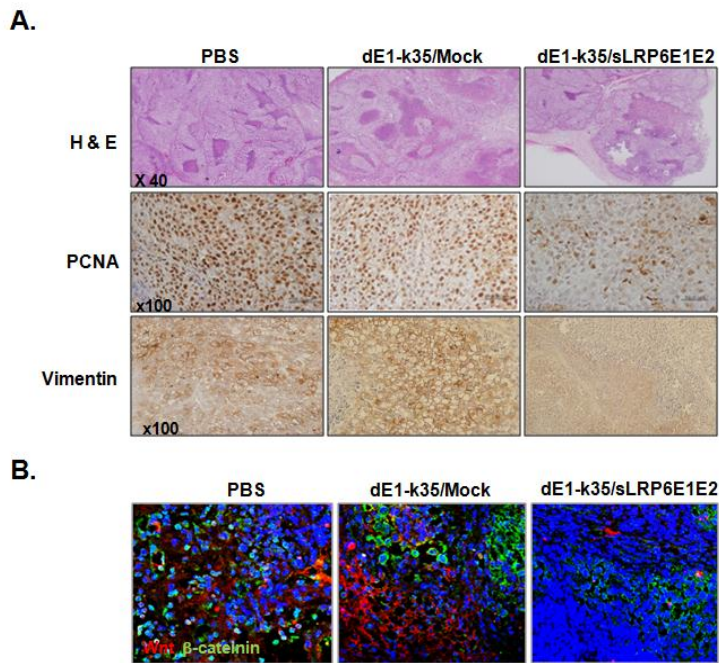


Figure 13. Decoy Wnt receptor sLRP6E1E2 are decreased enriched breast cancer cell for tumorigenicity (a) Histological and immunohistochemical analysis. Tumor tissues were collected from mice at 3 days after final treatment, and paraffin section of tumor tissue was stained with hematoxylin and eosin (H&E) (top rows, original magnification: $\times 40$). Tumor sections from each group were immunostained against anti-PCNA antibody (middle rows), anti-vimentin antibody (bottom rows), Original magnification: $\times 400$. (b) Cells were stained with DAPI (blue), anti-Wnt3a (red), or anti- β -catenin (green). Original magnification: $\times 200$.

13. Wnt treatment results altered cell morphology and induces EMT in tumor cells

EMT is an important process in tumor development, and the Wnt/ β -catenin signal pathway may play an important role in this process. Therefore, we investigated whether Wnt3a could induce EMT in H322 cells. We found that cells became elongated and spindle-shaped 1 day after Wnt3a treatment, resembling the morphology of mesenchymal cells (Fig. 14A). We also observed increased expression of mesenchymal markers Vimentin and β -catenin with a concomitant decrease in epithelial marker E-cadherin (Fig. 14B). Immunofluorescence staining revealed that actin and E-cadherin levels were dramatically reduced in cell–cell contacts after Wnt3a treatment (Fig. 14C).

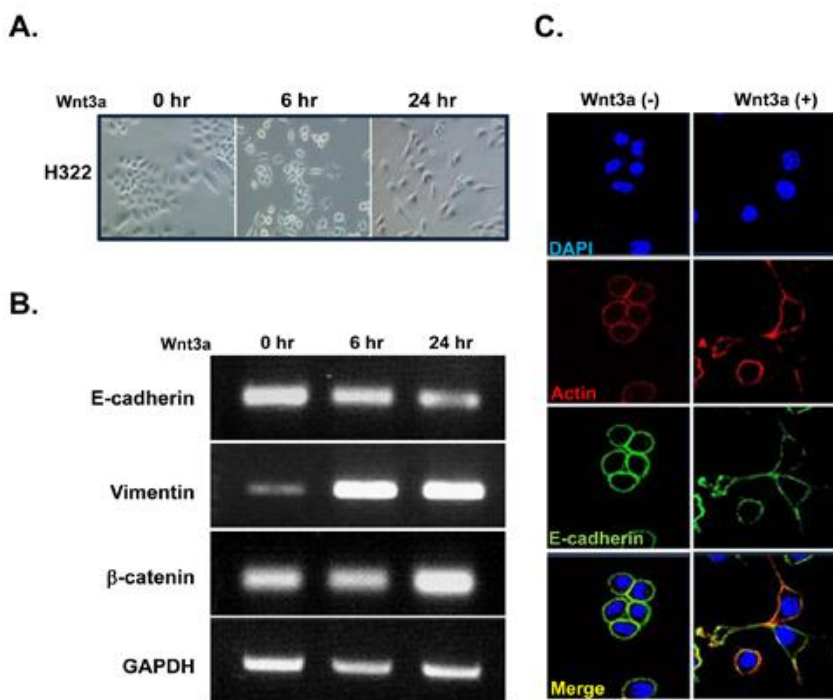


Figure 14. Wnt3a treatment results in the disruption of cell-cell junctions and epithelial-to-mesenchymal transition in tumor cells. (a) H322 cells were treated with Wnt3a (100 ng/ml) for the indicated times, and morphology changes were observed by light microscopy. Original magnification, $\times 200$. (b) E-cadherin, Vimentin, and β -catenin mRNA levels in H322 cells after Wnt3a treatment. (c) H322 cells were stained with DAPI (blue), TRITC-labeled actin (red), or anti E-cadherin (green) after 24 incubation with or without Wnt3a (100 ng/ml). Original magnification, $\times 630$

14. sLRP6E1E2 suppresses in vitro motility and invasiveness

Acquisition of migratory properties by cancer cells is important for metastatic tumor cell spread²⁷. Because increasing Wnt3a appeared to enhance motility and invasiveness, we asked whether interfering with the Wnt signaling pathway by expressing sLRP6E1E2 would inhibit *in vitro* motility and invasion. We examined the effect of sLRP6E1E2 on cancer cells using transwell motility and matrigel invasion assays. We collected conditioned medium from PBS-treated, dE1-k35/LacZ-transduced, and dE1-k35/sLRP6E1E2-transduced cells after treatment with or without Wnt3a. Conditioned medium from dE1-k35/sLRP6E1E2-transduced cells inhibited migration by 12.4% (without Wnt3a) and 23.8% (with Wnt3a) compared with conditioned medium from dE1-k35/LacZ-transduced cells ($P<0.001$) (Fig. 15A). Similarly, conditioned medium from dE1-k35/sLRP6E1E2-transduced cells inhibited invasion by 34.2% (without Wnt3a) and 56.2% (with Wnt3a) compared with conditioned medium from dE1-k35/LacZ-transduced cells (Fig. 15B). In breast cancer cells, conditioned medium from dE1-k35/sLRP6E1E2-transduced cells inhibited migration by 30.2% (SKBR3) and 38.3% (MDA-MB-468) compared with conditioned medium from dE1-k35/Mock-transduced cells ($P<0.01$) (Fig. 15C and 15D).

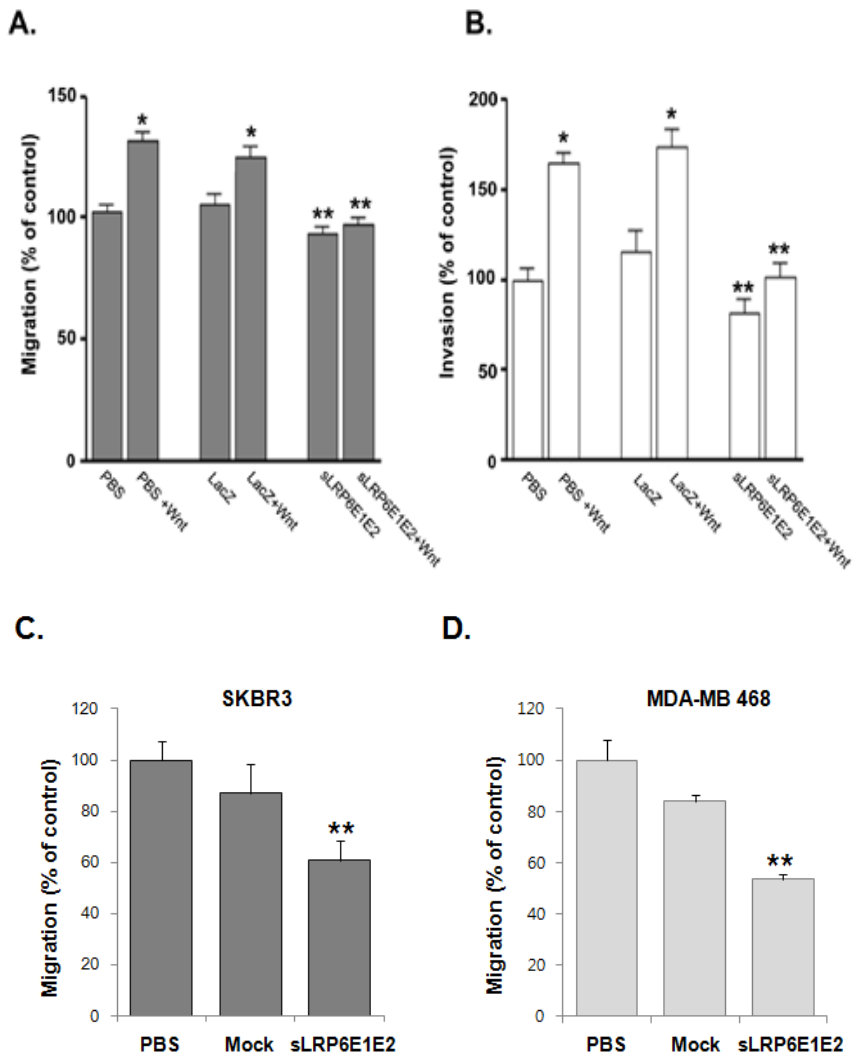


Figure 15. Inhibition of cancer cell migration and invasion by Decoy Wnt receptor sLRP6E1E2 (a) Quantitative analysis of A549 lung cancer cell migration. Experiments were performed in triplicate, and results are expressed as mean \pm SEM. * $P < 0.05$ versus PBS- or dE1-k35/LacZ-treated controls;

****P<0.001** versus PBS or dE1-k35/LacZ with Wnt3a. (b) Invasion of tumor cells was quantified as number of cells in five fields of view per filter. Experiments were performed in triplicate, and results are expressed as mean \pm SEM. ***P<0.05** versus PBS- or dE1-k35/LacZ-treated controls; ****P<0.001** versus PBS or dE1-k35/LacZ with Wnt3a. (c and d) Quantitative analysis of SKBR3 and MDA-MB-468 cells migration. Experiments were performed in triplicate, and results are expressed as mean \pm SEM. ****P<0.01** versus dE1-k35/Mock

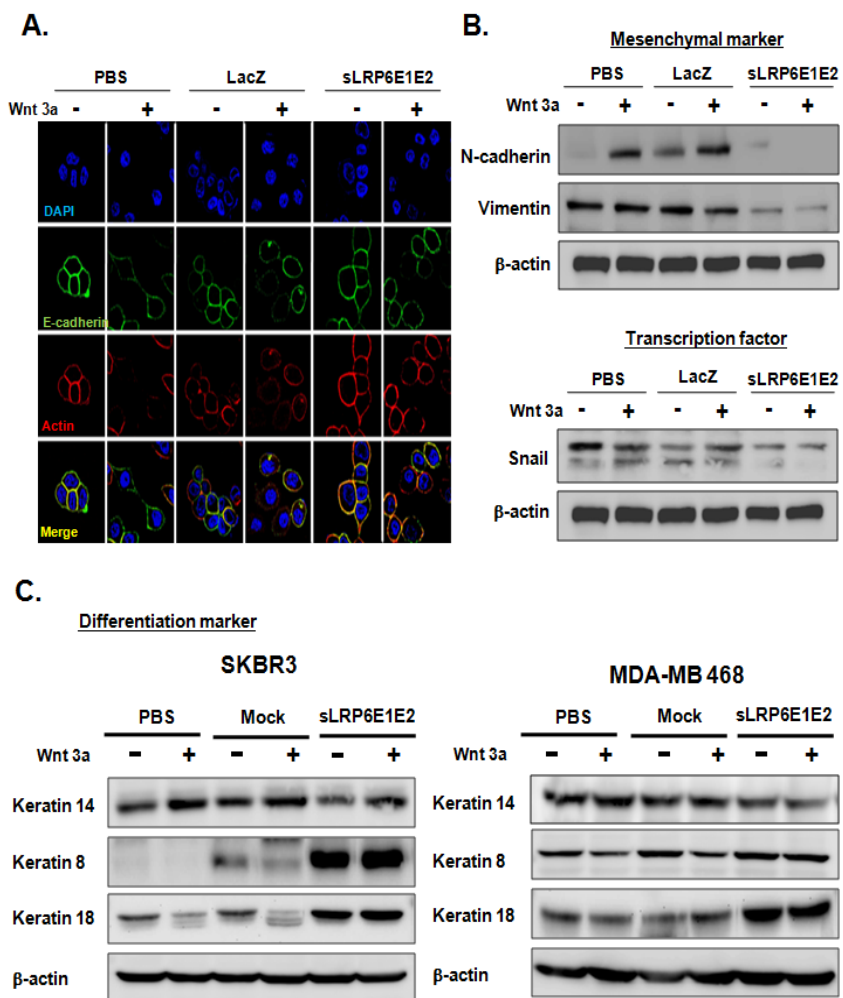
15. sLRP6E1E2 modulates EMT-related marker expression and MMP-2/MMP-9 activity

EMT has been shown to be important for cancer progression and metastasis. Therefore, we examined whether sLRP6E1E2 can modulate EMT-related markers associated with tumor invasion in H322 cell. Figure 16A showed that dE1-k35/sLRP6E1E2-transduced cells exhibited up-regulation of epithelial markers E-cadherin and actin by immunofluorescent staining. Conversely, mesenchymal markers (i.e., N-cadherin and vimentin) were markedly down-regulated in dE1-k35/sLRP6E1E2-transduced cells (Fig. 16B, upper panel). The expression of transcription factor Snail which is known to repress E-cadherin and promote a mesenchymal phenotype²⁸ was also down-

regulated (Fig. 16B, lower panel). In breast cancer cells, dE1-k35/sLRP6E1E2-transduced cells exhibited up-regulation of luminal makers (keratin 8 and keratin 18) with the differentiation of the cells and down-regulated basal/myoepithelial marker (cytokeratin 14) with the undifferentiated compared to those in PBS-treated and dE1-k35/Mock transduced cells after treatment with or without Wnt3a (Fig. 16C). The mesenchymal markers of β -catenin and vimentin was upregulated by Wnt3a treatment, but these levels were lower in dE1-k35/sLRP6E1E2-transduced cells compared to those in PBS-treated and dE1-k35/Mock transduced cells. Also, the expression of transcription factor Snail which is known to repress E-cadherin and promote a mesenchymal phenotype was down-regulated by sLRP6E1E2-transduced (Fig 16D). Together, these data further support the role of sLRP6E1E2 in modulating EMT-related events.

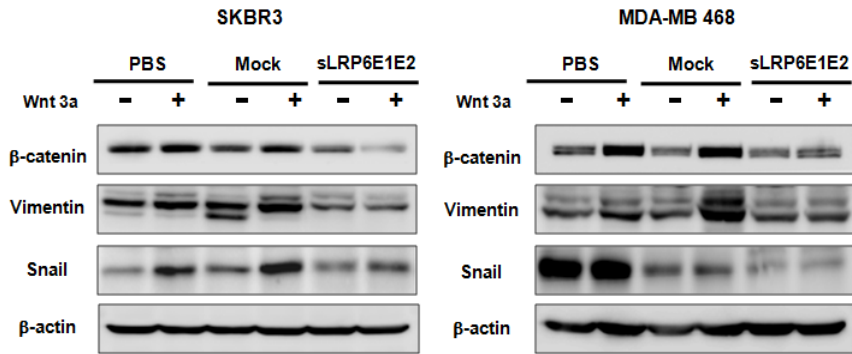
Several MMPs are additional Wnt target genes that play an important role in promoting invasion and metastasis of malignantly transformed cells^{29,30}. We therefore examined the effect of sLRP6E1E2 on expression of MMP-2 and MMP-9, which play a critical role in angiogenesis, tumor growth, and metastasis. As shown in Fig. 16E and F, Wnt3a stimulation upregulated MMP-2 and MMP-9 enzyme activity in PBS-treated and dE1-k35/LacZ-transduced A549 cells, but dE1-k35/sLRP6E1E2-transduced cells showed low

MMP-2 and MMP-9 enzyme activity with or without Wnt3a treatment. Taken together, these findings suggest that sLRP6E1E2 affected multiple Wnt-related pathways in human non-small cell lung cancer cell lines, leading to reduced cellular invasiveness.

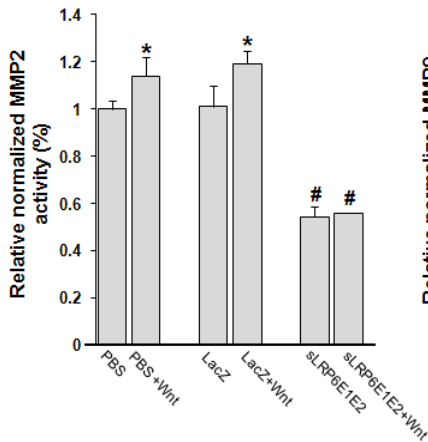


D.

Epithelial mesenchymal transition marker



E.



F.

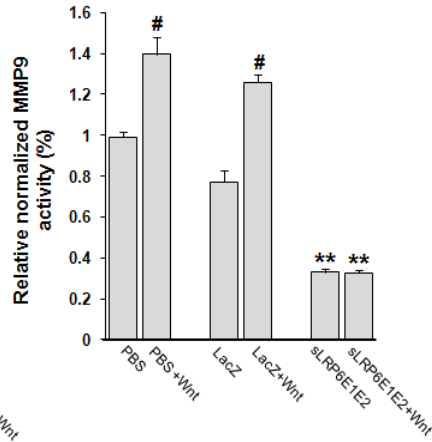


Figure 16. Decoy Wnt receptor sLRP6E1E2 modulates expression of epithelial-to-mesenchymal transition markers and MMPs. (a) Expression of EMT markers in H322 cells after 24 hr treatment with PBS, dE1-k35/LacZ, or dE1-k35/sLRP6E1E2 in the presence and absence of Wnt3a (100 ng/ml).

Cells were stained with DAPI (blue), TRITC-labeled actin (red), or anti E-cadherin (green). Original magnification, $\times 630$. (b) Expression of EMT-related markers in H322 cell lines. Expression levels of mesenchymal markers (N-cadherin & vimentin) as well as transcriptional factor (Snail) was determined by Western blotting. (c) Expression of differentiation markers in breast cancer cell lines. The western blot using specific antibodies against keratin 14, keratin 8 and keratin 18. (d) Expression of EMT-related markers in breast cancer cell lines. Expression of mesenchymal markers (β -catenin, vimentin), as well as transcriptional factors (Snail), was determined by Western blotting. (e and f) A549 cells were transduced with dE1-k35/LacZ or dE1-k35/sLRP6E1E2 with or without Wnt3a (100 ng/ml). The enzyme activity of MMP-2 and MMP-9 was measured in supernatants collected from transduced cells at 48 hr using the Sensolyte 520 MMP-2 and MMP-9 assay kit. Experiments were performed in triplicate, and results are expressed as mean \pm SEM. (d) $*P < 0.05$, (f) $^{\#}P < 0.01$ versus PBS- or dE1-k35/LacZ-treated controls; (d) $^{\#}P < 0.01$, (f) $**P < 0.001$ versus PBS or dE1-k35/LacZ with Wnt3a.

IV. DISCUSSION

Aberrant activation of the Wnt pathway contributes to human cancer progression³¹. Accordingly, monoclonal antibodies against Wnt ligands^{32,33} and overexpression of Wnt antagonists^{34,35} are able to reduce *in vivo* tumor growth. Members of the sFRP family bind directly to Wnts, inhibiting their ability to bind to the Wnt receptor complex. The Fzd8 soluble extracellular domain suppresses Wnt-driven tumor growth *in vivo*¹¹ and two sFRPs, FrzA and FrzB inhibited Wnt-1-mediated increase in cytoplasmic β -catenin levels, TCF transcriptional activity *in vitro*, and tumor growth and metastasis³⁶.

Antagonists that interfere with Wnt ligand/receptor interactions may therefore be potent cancer treatments. However, primary human tumors and cancer cell lines express multiple Wnt and Fzd receptors, and the specificity of Wnt proteins for the various receptors is unclear³⁶. Therefore, it is difficult to design a Wnt antagonist that can block these interactions. Recently, Lu et al. reported that cotransfection of vectors expressing Wnt3 and LRP6 receptor increased TCF activation³⁷, suggesting the therapeutic potential of a soluble LRP6 receptor as a Wnt antagonist. Therefore, we generated sLRP6E1E2 based on the LRP6 EGF repeats required for functional interaction with Wnt.

In the present study, we demonstrated that sLRP6E1E2 is secreted and binds specifically to Wnt3a, as evidenced by decreased endogenous

Wnt3a and LRP6 levels after transduction with sLRP6E1E2-expressing adenoviruses (Fig. 3). Wnt signaling affects multiple targets; therefore, we then assessed the effect of sLRP6E1E2 on pathways responsible for tumor growth, invasion, and metastasis. Our *in vitro* studies showed that sLRP6E1E2 reduced cell proliferation by inhibiting MEK-ERK and PI3K-Akt signaling (Fig. 7). Since PI3K-Akt signaling regulates cell survival and apoptosis³⁸, the ability of sLRP6E1E2 to induce apoptosis was assessed. As shown in Fig. 9, dE1-k35/sLRP6E1E2 transduction increased cytosolic cytochrome *c* levels, consistent with apoptosis through a mitochondria-dependent pathway.

Limitations of replication-incompetent adenoviruses for cancer therapy include nonselective delivery of therapeutic genes to both normal and tumor cells, and inability to replicate and spread to neighboring tumor cells. To improve the therapeutic value of adenovirus-mediated gene therapy, a cancer cell-specific replicating adenovirus (oncolytic adenovirus) has been developed³⁹. Our group previously developed RdB, an E1A-E1B double mutant oncolytic adenovirus with higher cancer cell-specific cytotoxicity and viral replication than E1A or E1B single mutant oncolytic adenoviruses⁴⁰. As shown in Fig. 10, tumors treated with RdB-k35/sLRP6E1E2 were 54% smaller than tumors treated with the oncolytic adenovirus not expressing

sLRP6E1E2 (RdB-k35) and 44% smaller than those treated with the non-replicating dE1-k35/sLRP6E1E2. RdB-k35/sLRP6E1E2 increased apoptosis, but also exerted anti-angiogenic effects. Immunostaining tumor tissues against CD31, a marker of angiogenesis, showed that the control oncolytic adenovirus RdB-k35 produced effects similar to that of RdB-k35/sLRP6E1E2. We and other groups previously demonstrated that replication-competent adenoviruses suppress tumor angiogenesis through the preserved E1A region ^{16,41,42}, indicating that sLRP6E1E2 expression from the vectors does not play a role in reducing tumor angiogenesis.

During tumor metastasis, disseminated cancer cells appear to require the ability to self-renew, similar to that exhibited by stem cells. Our results show that Wnt signaling upregulates EMT-related molecules Vimentin and β -catenin and increased tumor cell migration and invasion (Fig. 14). Cells were more compact and adhesive after treatment with the sLRP6E1E2-expressing adenovirus (data not shown), with increased expression of epithelial markers (E-cadherin and actin filaments) and down-regulation of mesenchymal markers (vimentin, N-cadherin, and Snail) (Fig. 13). Moreover, sLRP6E1E2 reduced expression of MMP-2/MMP-9, which correlate with tumorigenicity and metastatic potential of cancer cells ⁴³. Therefore, it is important to determine whether targeting Wnt ligand-receptor interactions

will reduce tumor recurrence and/or metastasis, warranting future investigation.

Many studies have demonstrated the association between aberrant expression of Wnt ligands/receptors and human cancer development/progression. The current study demonstrates for the first time that a decoy receptor consisting of LRP6 Wnt-binding domains can effectively inhibit Wnt signaling and downregulate potential Wnt targets. In addition, sLRP6E1E2 markedly reduced tumor growth, invasion, and EMT. Taken together, our findings demonstrate the therapeutic potential of sLRP6E1E2 as a novel cancer gene therapy. Ongoing studies in our laboratories are aimed at determining the efficacy of sLRP6E1E2 against cancer stem cells.

V. CONCLUSION

The current study demonstrates for the first time that a decoy receptor consisting of LRP6 Wnt-binding domains can effectively inhibit Wnt signaling and downregulate potential Wnt targets. In addition, sLRP6E1E2 markedly reduced tumor growth, invasion, and EMT. Taken together, our findings demonstrate the therapeutic potential of sLRP6E1E2 as a novel cancer gene therapy. Ongoing studies in our laboratories are aimed at determining the efficacy of sLRP6E1E2 against cancer stem cells.

REFERENCES

1. Polakis P. Wnt signaling and cancer. *Genes Dev* 2000;14:1837-51.
2. Burstein HJ, Gelber S, Guadagnoli E, Weeks JC. Use of alternative medicine by women with early-stage breast cancer. *N Engl J Med* 1999;340:1733-9.
3. Broxterman HJ, Georgopapadakou NH. Anticancer therapeutics: a surge of new developments increasingly target tumor and stroma. *Drug Resist Updat* 2007;10:182-93.
4. Liu JR, Opirari AW, Tan L, Jiang Y, Zhang Y, Tang H, et al. Dysfunctional apoptosome activation in ovarian cancer: implications for chemoresistance. *Cancer Res* 2002;62:924-31.
5. Nishio M, Koshikawa T, Kuroishi T, Suyama M, Uchida K, Takagi Y, et al. Prognostic significance of abnormal p53 accumulation in primary, resected non-small-cell lung cancers. *J Clin Oncol* 1996;14:497-502.
6. Nishio M, Koshikawa T, Yatabe Y, Kuroishi T, Suyama M, Nagatake M, et al. Prognostic significance of cyclin D1 and retinoblastoma expression in combination with p53 abnormalities in primary, resected non-small cell lung cancers. *Clin Cancer Res* 1997;3:1051-8.

7. Mitsudomi T, Kosaka T, Endoh H, Horio Y, Hida T, Mori S, et al. Mutations of the epidermal growth factor receptor gene predict prolonged survival after gefitinib treatment in patients with non-small-cell lung cancer with postoperative recurrence. *J Clin Oncol* 2005;23:2513-20.
8. Nusse R, Theunissen H, Wagenaar E, Rijsewijk F, Gennissen A, Otte A, et al. The Wnt-1 (int-1) oncogene promoter and its mechanism of activation by insertion of proviral DNA of the mouse mammary tumor virus. *Mol Cell Biol* 1990;10:4170-9.
9. Beachy PA, Karhadkar SS, Berman DM. Tissue repair and stem cell renewal in carcinogenesis. *Nature* 2004;432:324-31.
10. Holcombe RF, Marsh JL, Waterman ML, Lin F, Milovanovic T, Truong T. Expression of Wnt ligands and Frizzled receptors in colonic mucosa and in colon carcinoma. *Mol Pathol* 2002;55:220-6.
11. DeAlmeida VI, Miao L, Ernst JA, Koeppen H, Polakis P, Rubinfeld B. The soluble wnt receptor Frizzled8CRD-hFc inhibits the growth of teratocarcinomas in vivo. *Cancer Res* 2007;67:5371-9.
12. Li Y, Lu W, He X, Schwartz AL, Bu G. LRP6 expression promotes cancer cell proliferation and tumorigenesis by altering beta-catenin subcellular distribution. *Oncogene* 2004;23:9129-35.

13. Liu CC, Pearson C, Bu G. Cooperative folding and ligand-binding properties of LRP6 beta-propeller domains. *J Biol Chem* 2009;284:15299-307.
14. He X, Semenov M, Tamai K, Zeng X. LDL receptor-related proteins 5 and 6 in Wnt/beta-catenin signaling: arrows point the way. *Development* 2004;131:1663-77.
15. Zhang Y, Wang Y, Li X, Zhang J, Mao J, Li Z, et al. The LRP5 high-bone-mass G171V mutation disrupts LRP5 interaction with Mesd. *Mol Cell Biol* 2004;24:4677-84.
16. Yoo JY, Kim JH, Kwon YG, Kim EC, Kim NK, Choi HJ, et al. VEGF-specific short hairpin RNA-expressing oncolytic adenovirus elicits potent inhibition of angiogenesis and tumor growth. *Mol Ther* 2007;15:295-302.
17. Yun CO, Kim E, Koo T, Kim H, Lee YS, Kim JH. ADP-overexpressing adenovirus elicits enhanced cytopathic effect by induction of apoptosis. *Cancer Gene Ther* 2005;12:61-71.
18. Yoo JY, Kim JH, Kim J, Huang JH, Zhang SN, Kang YA, et al. Short hairpin RNA-expressing oncolytic adenovirus-mediated inhibition of IL-8: effects on antiangiogenesis and tumor growth inhibition. *Gene Ther* 2008;15:635-51.

19. Forrester WC. The Ror receptor tyrosine kinase family. *Cell Mol Life Sci* 2002;59:83-96.
20. Signorello LB, Cohen SS, Bosetti C, Stovall M, Kasper CE, Weathers RE, et al. Female survivors of childhood cancer: preterm birth and low birth weight among their children. *J Natl Cancer Inst* 2006;98:1453-61.
21. Yoon AR, Kim JH, Lee YS, Kim H, Yoo JY, Sohn JH, et al. Markedly enhanced cytolysis by E1B-19kD-deleted oncolytic adenovirus in combination with cisplatin. *Hum Gene Ther* 2006;17:379-90.
22. Korinek V, Barker N, Morin PJ, van Wichen D, de Weger R, Kinzler KW, et al. Constitutive transcriptional activation by a beta-catenin-Tcf complex in APC^{-/-} colon carcinoma. *Science* 1997;275:1784-7.
23. Yun MS, Kim SE, Jeon SH, Lee JS, Choi KY. Both ERK and Wnt/beta-catenin pathways are involved in Wnt3a-induced proliferation. *J Cell Sci* 2005;118:313-22.
24. Kim SE, Lee WJ, Choi KY. The PI3 kinase-Akt pathway mediates Wnt3a-induced proliferation. *Cell Signal* 2007;19:511-8.

25. Grotewold L, Ruther U. The Wnt antagonist Dickkopf-1 is regulated by Bmp signaling and c-Jun and modulates programmed cell death. *EMBO J* 2002;21:966-75.
26. Yang L, Mashima T, Sato S, Mochizuki M, Sakamoto H, Yamori T, et al. Predominant suppression of apoptosome by inhibitor of apoptosis protein in non-small cell lung cancer H460 cells: therapeutic effect of a novel polyarginine-conjugated Smac peptide. *Cancer Res* 2003;63:831-7.
27. Gupta GP, Massague J. Cancer metastasis: building a framework. *Cell* 2006;127:679-95.
28. Yang J, Weinberg RA. Epithelial-mesenchymal transition: at the crossroads of development and tumor metastasis. *Dev Cell* 2008;14:818-29.
29. Wu B, Crampton SP, Hughes CC. Wnt signaling induces matrix metalloproteinase expression and regulates T cell transmigration. *Immunity* 2007;26:227-39.
30. Bjornland K, Flatmark K, Pettersen S, Aaasen AO, Fodstad O, Maelandsmo GM. Matrix metalloproteinases participate in osteosarcoma invasion. *J Surg Res* 2005;127:151-6.

31. Uematsu K, He B, You L, Xu Z, McCormick F, Jablons DM. Activation of the Wnt pathway in non small cell lung cancer: evidence of dishevelled overexpression. *Oncogene* 2003;22:7218-21.
32. He B, You L, Uematsu K, Xu Z, Lee AY, Matsangou M, et al. A monoclonal antibody against Wnt-1 induces apoptosis in human cancer cells. *Neoplasia* 2004;6:7-14.
33. You L, He B, Xu Z, Uematsu K, Mazieres J, Fujii N, et al. An anti-Wnt-2 monoclonal antibody induces apoptosis in malignant melanoma cells and inhibits tumor growth. *Cancer Res* 2004;64:5385-9.
34. Vincan E, Darcy PK, Smyth MJ, Thompson EW, Thomas RJ, Phillips WA, et al. Frizzled-7 receptor ectodomain expression in a colon cancer cell line induces morphological change and attenuates tumor growth. *Differentiation* 2005;73:142-53.
35. Zi X, Guo Y, Simoneau AR, Hope C, Xie J, Holcombe RF, et al. Expression of Frzb/secreted Frizzled-related protein 3, a secreted Wnt antagonist, in human androgen-independent prostate cancer PC-3 cells suppresses tumor growth and cellular invasiveness. *Cancer Res* 2005;65:9762-70.

36. Dennis S, Aikawa M, Szeto W, d'Amore PA, Papkoff J. A secreted frizzled related protein, FrzA, selectively associates with Wnt-1 protein and regulates wnt-1 signaling. *J Cell Sci* 1999;112 (Pt 21):3815-20.
37. Lu D, Zhao Y, Tawatao R, Cottam HB, Sen M, Leoni LM, et al. Activation of the Wnt signaling pathway in chronic lymphocytic leukemia. *Proc Natl Acad Sci U S A* 2004;101:3118-23.
38. Franke TF, Hornik CP, Segev L, Shostak GA, Sugimoto C. PI3K/Akt and apoptosis: size matters. *Oncogene* 2003;22:8983-98.
39. Kurihara T, Brough DE, Kovesdi I, Kufe DW. Selectivity of a replication-competent adenovirus for human breast carcinoma cells expressing the MUC1 antigen. *J Clin Invest* 2000;106:763-71.
40. Kim J, Kim JH, Choi KJ, Kim PH, Yun CO. E1A- and E1B-Double mutant replicating adenovirus elicits enhanced oncolytic and antitumor effects. *Hum Gene Ther* 2007;18:773-86.
41. Zhou Z, Zhou RR, Guan H, Bucana CD, Kleinerman ES. E1A gene therapy inhibits angiogenesis in a Ewing's sarcoma animal model. *Mol Cancer Ther* 2003;2:1313-9.
42. Saito Y, Sunamura M, Motoi F, Abe H, Egawa S, Duda DG, et al. Oncolytic replication-competent adenovirus suppresses tumor

angiogenesis through preserved E1A region. *Cancer Gene Ther* 2006;13:242-52.

43. Sato H, Kida Y, Mai M, Endo Y, Sasaki T, Tanaka J, et al. Expression of genes encoding type IV collagen-degrading metalloproteinases and tissue inhibitors of metalloproteinases in various human tumor cells. *Oncogene* 1992;7:77-83.

ABSTRACT (IN KOREAN)

Wnt수용체 soluble LRP6 E1E2 발현에 따른 종양 형성과

세포의 침습 억제

<지도교수 허만옥>

연세대학교 대학원 의과학과

이정선

암은 세계적으로 가장 많은 사망자를 내는 질병 중의 하나
로써, 암에 대한 치료는 외과적 수술이나 방사선치료 또는 항암제와
같은 표준치료가 사용되고 있지만 암의 재발에 의한 근본적인 치료
에는 한계가 있다. 최근에 암에 대한 다양한 분자적 메커니즘의 이
해가 증가되면서 암에 대한 새로운 치료법을 개발 하고자 하는 노
력들이 이루어져 왔다. 특히 다양한 항암제의 개발로 악성 종양을
가진 환자들의 생존율을 증가시켰지만 여전히 항암제의 내성은 암
의 치료에 있어 가장 큰 실패의 원인으로 보고되고 있다. 왜냐 하면,

많은 악성 종양은 다양한 암과 관련된 유전자, 즉 Wnt, K-ras, extracellular signal-regulated kinase (ERK), 그리고 Akt 와 같은 유전자가 변형되어 있어 다양한 암에서의 서로 다른 분자적 신호전달을 가지고 있는것으로 보여지고 있다.

암에서의 Wnt의 역할은 20년전 Wnt1이 MMTV에 의해 생성된 마우스 유방에서 바이러스가 삽입되어 활성화되는 암 유전자로 처음 밝혀졌다. 최근 세포 내 Wnt 신호전달의 이상이 암 발생에 밀접하게 관여 하며, 특히 Wnt의 수용체와 리간드 그리고 길항자 (antagonist)의 변형은 암의 발달 및 악성도와 연관되어 있다고 보고되어 있다. Wnt수용체인 Frizzled과 LRP5/6는 폐암과 유방암에서 과 발현되 있지만, 이와 반대로 Wnt 길항자인 (Wnt inhibitory factor-1 (WIF-1), secreted Frizzled-related proteins (sFRP) and dickkopf proteins (DKK))는 억제 되어 있거나 낮은 활성화를 보이고 있다. 그러므로 Wnt의 억제자인 sFRP1(secreted Frizzled-related protein 1)을 과 발현시키므로써 종양의 성장을 억제하거나 또 다른 Wnt의 길항자인 Dkk1과 WIF-1을 이용하므로써 Wnt와의 선택적 결합을 통한 Wnt신호전달을 억제함으로써 암을 치료하는 연구가 이루어져 왔다. 선행연구 결과를 바탕으로 본 실험에서는 Wnt와 수용체의 결합을 차단함으로써 암의 발생을 억제할 수 있는 새로운 효과적인 치료용 물질을 찾고자 하였다.

LRP6는 LDLR의 type I 세포막 단백질로써 Wnt신호전달의 중요한 수용체이다. LRP6의 세포막의 부위는 총 4개의 epidermal growth factor (EGF)-like 반복 부위를 가지고 있다. 이중 첫 번째와 두 번째 도메인은 Wnt와 특이적으로 결합하고 세 번째와 네 번째 도메인은 DKK1와 결합할 수 있는 생물학적 특성을 가지고 있다. 본 연구에서는 Wnt를 선택적으로 차단하기 위하여 Wnt의 수용체인 LRP6의 4개의 반복된 epidermal growth factor(EGF) 도메인 중 Wnt와 결합하는 도메인만을 발현하는 유전자인 E1E2를 선택하였다. 또한 생체 내 유전자 전달 효율을 증가시키고, 장기간 발현 및 종양세포에 특이적으로 발현하기 위하여 sLRP6E1E2를 탑재한 복제불능 아데노바이러스 dE1-k35/sLRP6E1E2와 종양 선택적 살상 아데노바이러스 RdB-k35/sLRP6E1E2를 각각 제작하였다. 제작된 sLRP6E1E2는 효과적으로 β -catenin의 핵안으로의 이동을 억제하였고, 또한 Wnt/ β -catenin의 세포 신호전달 및 암세포의 증식 역시 효과적으로 차단하였다. 이 결과는 sLRP6E1E2가 Wnt에 의한 MEK-ERK 그리고 PI3K-Akt 신호전달을 억제한다는 것을 확인하였다. 이런 sLRP6E1E2는 다양한 폐암세포주에서 세포고사 현상을 보였으며, 특히 세포고사의 대표적인 분자인 PARP, caspase-3, cytochrome-c 발현이 모두 증가함을 관찰하였다. 앞선 결과는 폐

암세포주 뿐만 아니라 유방암 세포주를 이용한 항종양 실험에서도 우수한 항종양 효과를 보임을 확인하였다. 또한 조직면역염색을 통하여, sLRP6 E1E2에 의하여 세포의 성장이 억제되고 세포고사가 증가함을 보였고, Wnt/ β -catenin의 발현이 종양 조직내에 감소함을 관찰하였다. 게다가, sLRP6 E1E2는 EMT 관련된 다양한 유전자의 발현에도 영향을 주므로써, 세포의 이동능력의 감소에 효과적임을 알 수 있다.

본 연구는 처음으로 LRP6의 특이적인 Wnt 결합도메인을 이용하여 Wnt가 과발현 되어 있는 폐암세포주와 유방암 세포주에서 Wnt의 신호전달 및 타겟 유전자의 억제를 관찰하였다. 특히 sLRP6 E1E2에 의한 종양 성장, 전이, 그리고 EMT의 현상이 상당히 억제되었으며, 이는 암줄기세포의 치료 가능성을 보여주었다. 이런 결과는 새로운 암치료 유전자인 sLRP6 E1E2의 치료적 가능성을 설명해 준다.

핵심 되는 말: Wnt, soluble Wnt decoy receptor, LRP6, 상피세포에서 중간엽으로의 이행 (EMT), 세포의 고사,

PUBLICATION LIST

1. A Novel sLRP6E1E2 Inhibits Canonical Wnt Signaling, Epithelial-to-Mesenchymal Transition, and Induces Mitochondria-Dependent Apoptosis in Lung Cancer.

Lee JS, Hur MW, Lee SK, Choi WI, Kwon YG, Yun CO.

PLoS One. 2012;7(5):e36520. Epub 2012 May 14.

2 Soluble Vascular Endothelial Growth Factor Decoy Receptor FP3 Exerts Potent Antiangiogenic Effects.

Yu DC, **Lee JS**, Yoo JY, Shin H, Deng H, Wei Y, Yun CO.

Mol Ther. 2012 May;20(5):938-47. doi: 10.1038/mt.2011.285.

3. Negative Regulation-Resistant p53 Variant Enhances Oncolytic Adenoviral Gene Therapy.

Koo T, Choi IK, Kim M, **Lee JS**, Oh E, Kim J, Yun CO.

Hum Gene Ther. 2012 Feb 21. [Epub ahead of print]

4. Evolution of oncolytic adenovirus for cancer treatment.

Choi JW, **Lee JS**, Kim SW, Yun CO.

Adv Drug Deliv Rev. 2012 Jun 1;64(8):720-9. Epub 2011 Dec 24.

5. Linearized oncolytic adenoviral plasmid DNA delivered by bioreducible polymers.

Kim J, Kim PH, Nam HY, **Lee JS**, Yun CO, Kim SW.

J Control Release. 2012 Mar 28;158(3):451-60. Epub 2011 Dec 20

6. Oncolytic adenovirus co-expressing IL-12 and IL-18 improves tumor-specific immunity via differentiation of T cells expressing IL-12R β 2 or IL-18R α .

Choi IK, Lee JS, Zhang SN, Park J, Sonn CH, Lee KM, Yun CO.

Gene Ther. 2011 Sep;18(9):898-909